# AN INVESTIGATION OF CHANGING WIND ENERGY ON THE EVOLUTION OF COPANOBAY, TEXAS

By

BENJAMIN TAYLOR TROIANI

Bachelor of Science in Geology

Wichita State University

Wichita, Kansas

2006

Submitted to the Faculty of the
Graduate College of the
Oklahoma State University
in partial fulfillment of
the requirements for
the Degree of
MASTER OF SCIENCE
May, 2010

AN INVESTIGATION OF CHANGING WIND ENERGY

ON THE EVOLUTION OF COPANO BAY, TEXAS

Thesis Approved:

Dr. Alexander Simms

Thesis Adviser

Dr. Estella Atekwana

Dr. James Puckette

Dr. A. Gordon Emslie

Dean of the Graduate College

ACKNOWLEDGMENTS

This thesis exists as a result of the support provided by Boone Pickens School of Geology, Oklahoma State University. Without their financial support and use of their facilities, this thesis would not be possible. My advisor Dr. Alexander R. Simms deserves special credit. I feel he went above and beyond his duties as an advisor and was always there for guidance, support, and encouragement. Without his service, I would have never finished. I would also I like to thank the other members of my committee, Dr. James Puckette and Dr. Estella Atekwana for providing valuable input into my research.

I would like to thank Dr. Tim Dellapenna and Erin Weaver at Texas A&M at Galveston for providing the seismic data from Copano Bay and use of their facilities to help interpret the seismic data. I am very grateful for Yusuke Yokoyama from the University of Tokyo, Japan for providing radiocarbon ages. I would also like to thank Tyler Treece and Derk Federko for their help in the field and Lauren Miller for her help in the lab.

This research was funded by Gulf Coast Section of Economic Paleontologist and Mineralogists (GCSSEPM) Ed Picou fellowship for graduate students and the Petroleum Research Fund of the America Chemical Society.

# TABLE OF CONTENTS

LIST OF TABLES

LIST OF FIGURES

Figure | Page

# CHAPTER I

# INTRODUCTION

Estuaries are complex, dynamic, and sensitive not only to changes in sea-level rise but also to other factors including changes in sediment supply and climate (Allen, 1971; Shideler, 1984; Dalrymple et al., 1992; Rodriguez et al., 2005; Anderson et al., 2008; Maddox et al., 2008; Milliken et al., 2008b; Simms et al., 2008). One very important and often overlooked aspect of climate change is the impact that changing wind energy has on bay evolution. Shideler (1984) determined that wind is the dominant forcing agent regulating estuarine sedimentary processes along the Texas Gulf coast. Wind generated waves and currents, i.e. bottom wave orbitals, have the ability to resuspend bay-floor sediments in the water-column and a direct relationship exists between mean wind speed and sediment concentration in the water-column (Shideler, 1984). Bay-floor sediment concentration in the water column is a function of maximum bottom orbital velocity, which can be expressed by Lamp (1945) in the following equation.

$$U=H\pi/((T\sinh)((2\pi h)/\lambda))) \qquad \text{Eq. (1)}$$

Where $U$=the maxium bottom orbital velocity, $H$=the wave height, $T$=the wave period , $\lambda$=the wavelength, and $h$=water depth at the point of consideration. These wave parameters are controlled by the fetch of a bay and wind speed.

Shideler (1984) noticed that the resuspended bay-flood sediments within Nueces Bay, Texas were being exported out of the bay by strong northerly winds and the astronomical ebb tide. As a result of the resuspension of bay-flood sediments, estuarine systems are flushed of fine-grain bay-floor sediments. Price (1947) and Nichols (1989) noticed that sedimentation and accumulation rates along with lagoonal surface area (ie. fetch) are in equilibrium with wave energy dissipation. This relationship holds true for the bays of the Texas coast (Figure 1). Thus, changes in wind strength and/or fetch area will disrupt this equilibrium and cause a change in the accumulation rate of sediments within estuaries. In most modern lagoons, Nichols (1989) noticed that sediment accumulation rates equal the rate of relative sea-level rise.

The objective of this investigation is to study the role wind energy had on the evolution of Copano Bay over the last 10 k.a., a time of known variable sea-level rise, sediment supply, and climate (Allen, 1971; Shideler, 1984; Toomey et al., 1993; Tornqvist et al., 2004; Milliken et al., 2008a). With recent attention given to concerns of increased sea-level rise and changing climate patterns, the findings of this study will aid in the prediction of the response of estuaries to future changes in sea-level rise, climate, and sediment supply.

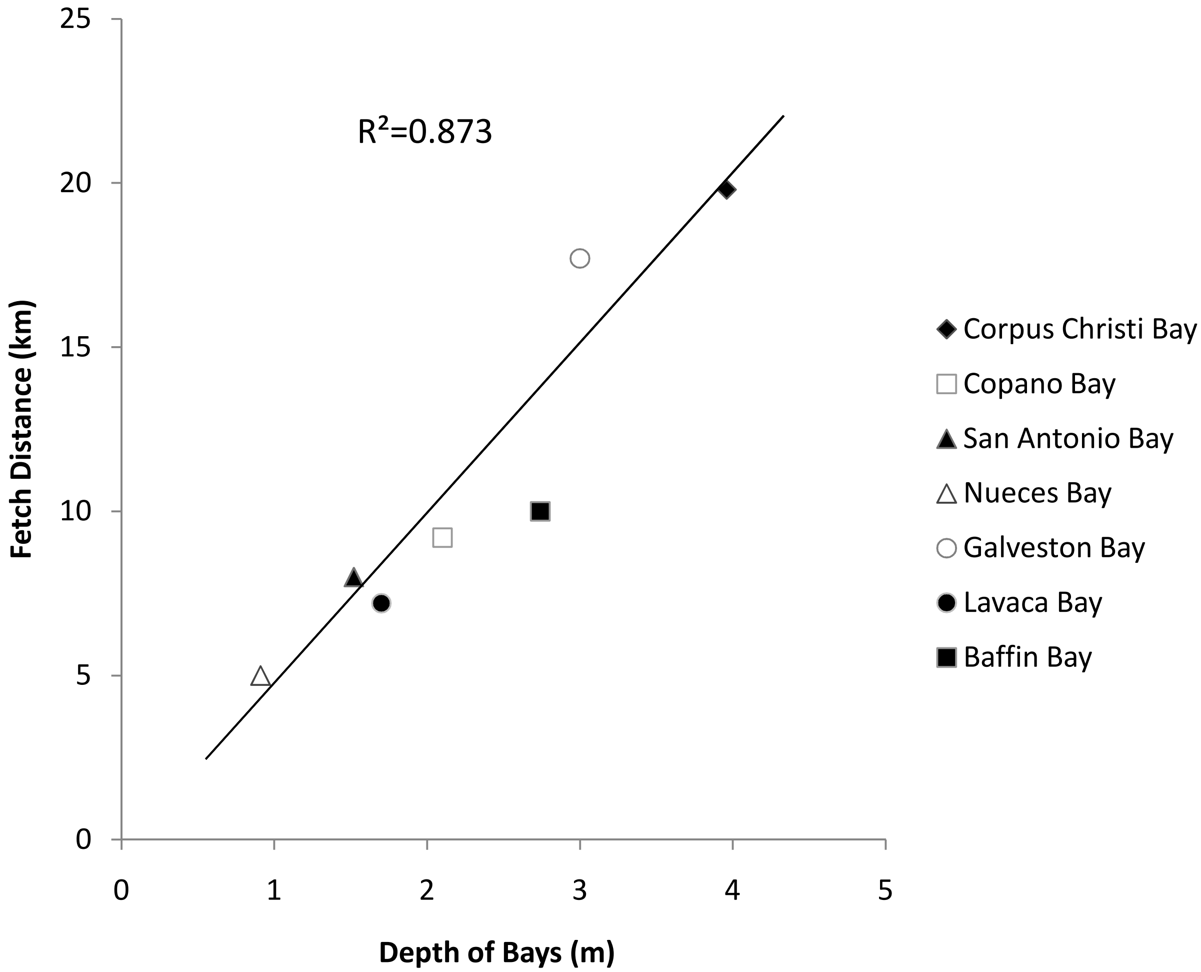


**Figure 1.** Graph showing a linear relationship between fetch and depth of the bays along the Texas Gulf Coast. See figure 2 for bay locations.

Our central hypothesis is that changes in wind energy during the Holocene impact the evolution of the bay and are recorded in the sedimentary deposits of Copano Bay, Texas. We test our hypothesis by documenting and describing the Holocene history of Copano Bay by presenting a three-dimensional model of Holocene sediments within the bay. A detailed grain-size analysis of Holocene middle-bay sediments is presented to document changes in wind energy and determine what impacts, if any, these changes had on the evolution of Copano Bay. Radiocarbon dates are used to constrain the timing of flooding and to determine the sedimentation rates within the bay.

As hurricanes also play a very important role in sedimentation along the Gulf of Mexico. Copano Bay was chosen as the study site due to its isolation with respect to the sea. Copano Bay is protected from the ocean by St. Joseph Island, Redfish Bay and Live Oak Peninsula (Figure 2). The closest connection with the open Gulf of Mexico is Aransas Pass, which is about 30 km to the south (Figure 2). Due to Copano Bay's isolation and orientation, the bay is protected during times of tropical storms and hurricanes. In addition, Live Oak Peninsula has a high enough profile, average elevation of 7 m, to prevent large scale wash-over of sand into the bay during times of storms, which may cause bias in any grain-size based proxy records of wind energy.

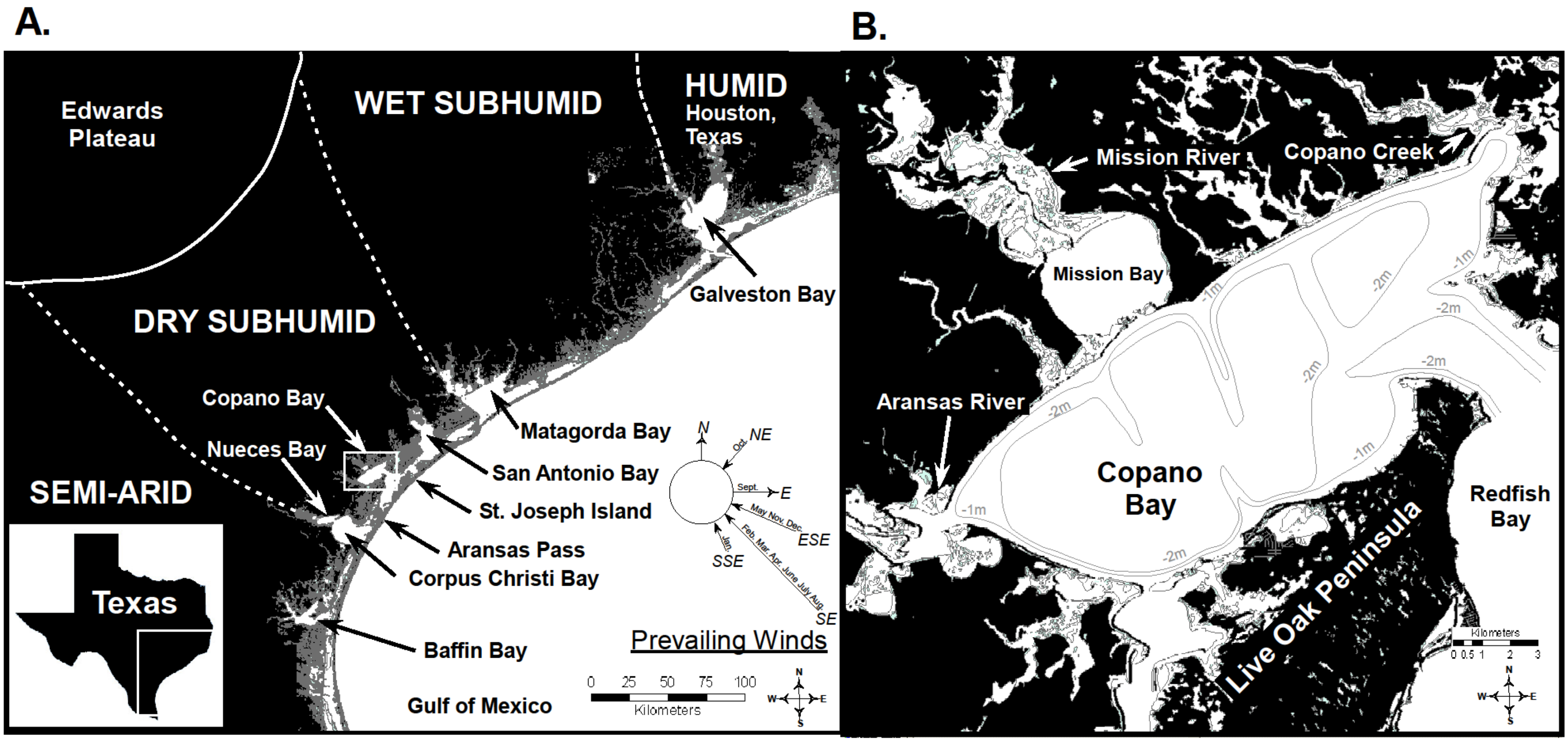


**Figure 2. A.** Map of Copano Bay in relation to local features including climatic belts and prevailing winds for the Gulf of Mexico modified from Thornthwaite (1948) Lohse (1955) **B.** Copano Bay including modern bathymetry and local features.

# CHAPTER II

# STUDY AREA

Copano Bay is located along the central Texas coast of the northwestern Gulf of Mexico (Figure 2). The central Texas coast represents a passive margin with a gentle coastal-plain. The average coastal-plain gradient is 0.75 m/km, and the continental-shelf gradient is 3 m/km (Simms et al., 2008). The long-term subsidence rates in the Copano Bay area are very low, averaging less than 0.05 mm/yr (Paine, 1993).

Copano Bay is aligned parallel to the present coast line of the Gulf of Mexico (Figure 2). The bay covers an area of approximately 168 $km^2$. Water depths reach 0.6-2.7 m but nearly 75% of the bay has a depth of 2.1 m (Figure 2). Live Oak Peninsula, Aransas Bay, and St. Joseph Island separate Copano Bay from the Gulf of Mexico (Figure 2). Copano Bay has three primary sources of freshwater: the Mission River, the Aransas River, and Copano Creek (Figure 2b). The average freshwater discharge from April 1981 through September 2005 was 4.5 $m^3/s$ for the Mission River, 1.2 $m^3/s$ for the Aransas River, and 1.3 $m^3/s$ for Copano Creek (United States Geological Survey, 2005).

Copano Bay is defined as a shallow, restricted, micro-tidal estuary typical of the Gulf Coast of Texas (Calnan, 1980). The bay lies within a sub-humid to semi-arid climate zone (Thornthwaite, 1948) with evaporation exceeding precipitation. Martinez-Andrade et al. (2005) indicated that from August 1981 to August 2005 the average salinity was 11.84‰ and the average water temperature was 25°C. The prevailing winds are onshore from the southeast and are most consistent during the late spring to early fall. During the late fall to early spring, the winds frequently have strong northerly components directed offshore (Figure 2a). These relatively high-speed winds are generally associated with "northerns", storms that frequently occur during the winter months when cold fronts pass southward into the Gulf of Mexico (Shideler, 1984). The average astronomical tidal range is less than 0.6 m in most tidal passes and decreases to 0.2 m in most of the bays on the Texas Gulf Coast (McGowen and Brewton, 1975). However, prevailing winds have significant fetch across most bays, resulting in wave set-up and wind tides generated by wind shear on the free-water surface. This can raise water levels by as much as 0.6 m above normal high tide levels along the windward bay margins (McGowen and Brewton, 1975).

Copano Bay is the flooded late Pleistocene/Holocene incised valley created by the Mission and Aransas Rivers and Copano Creek (Wright, 1980). During a sea-level fall between 120-20 ka, the rivers and creeks cut an incised valley 21 m deep (Wright, 1980). Major fluvial sediments are supplied to the bay by the Mission and Aransas River (Wright, 1980). Copano Bay represents an "under-filled" incised valley as defined by Simms et al. (2006) and is the site of a well preserved section of Holocene shallow marine sediments.

## Holocene Sea-Level History of the U.S. Gulf Coast:

The Holocene sea-level history of the Texas Gulf coast has been extensively studied: however, debate continues over some details. During the Last Glacial Maximum (LGM), which occurred 20,000 years ago, sea level along the Texas Gulf coast was 90 to 120 m lower than present (Shepard, 1956; Curray, 1960; McFarland, 1961; Nelson and Bray, 1970; Tornqvist et al., 2004; Simms et al., 2007). Controversy arises as to whether the postglacial rise was continuous or episodic. McFarland (1961) and Shepard (1956) believe that postglacial rise was continuous while Nelson and Bray (1970), Thomas and Anderson (1994), and Tornqvist et al. (2004) suggest that the overall rise was punctuated by brief periods of rapid sea-level rise around 15, 11, 9, and 8.2 ka. A study by Rodriguez et al. (2005) in the Trinity incised valley suggests that some Holocene sea-level events might have been the result of other mechanisms, such as the flooding of flat antecedent topography. The work of Simms et al. (2008) in Corpus Christi and Nueces bay suggest that other flooding events might have been the result of Holocene climatic changes, which resulted in a decrease in sediment delivery to the bay.

Recent studies of coral-based eustatic sea-level changes indicate two rapid increases in the rate of sea-level rise occurring at 14.5 and 11.3 ka (Lightly et al., 1982). These pulses are believed to be the result of rapid melting of the ice sheets and are known as meltwater pulse 1A and meltwater pulse 1B (Fairbanks, 1989; Bard et al., 1996). In addition, there is some discussion on whether sea level was ever higher then present during the mid Holocene. Curray (1960), Nelson and Bray (1970), Tornqvist et al. (2004), and Simms et al. (2007) suggest that within the U.S. Gulf coast, sea-level rose some 3-5 m over the last 5 k.y. and is presently at its highest position since the LGM.

Morton et al. (2000) and Blum et al. (2003) suggest sea level was up to 2 m higher during the mid-Holocene based on raised marine beach-ridges that rise 1.5-3 m above present sea level documented in Copano Bay, TX and along the Alabama Gulf coast. However, Donnelly and Giosan (2008) suggest the raised beach-ridges may be the result of heightened tropical cyclone activity accompanied with large storm surges. In addition, a more recent study by Simms et al. (2009) examined the elevation of ponds between an elevation of -0.8 m and 0.8 m in South Texas and found no evidence for higher than present sea level over the last 5.6 ka. For the purpose of this study, we will refer to the most recent sea-level curve proposed by Simms et al. (2007) (Figure 3).

## **Holocene Climate History:**

The climate during the Holocene in Texas has been a period of warming over the last 11 ka. The reconstruction of Holocene climate comes from a variety of sources including: vertebrate fossils, pollen, plant macrofossils, and stable carbon isotope analysis. A study of isotopes by Nordt et al.(1994) reveals a shift in the ratio of C3 to C4 plants during the *Early Holocene* (11 and 8 ka.) suggesting a time of transition between a cooler and wetter late Pleistocene and warmer and dryer Holocene climates. This interpretation is based on a 65 to 70% increase in the abundance of C4 plant biomass. This interpretation agrees with the study of Toomey et al (1993) who noticed the replacement of small vertebrate fossils that require high moisture by species that are more adapted to desert conditions in Hall’s Cave, Texas. In Hinds Cave, Texas, pollen records from the *Middle Holocene* (8.7 to 6 ka.) show significant amounts of xerophytic taxa such as *Agave* sp. and *Dasylirion* sp., which indicate desert like conditions

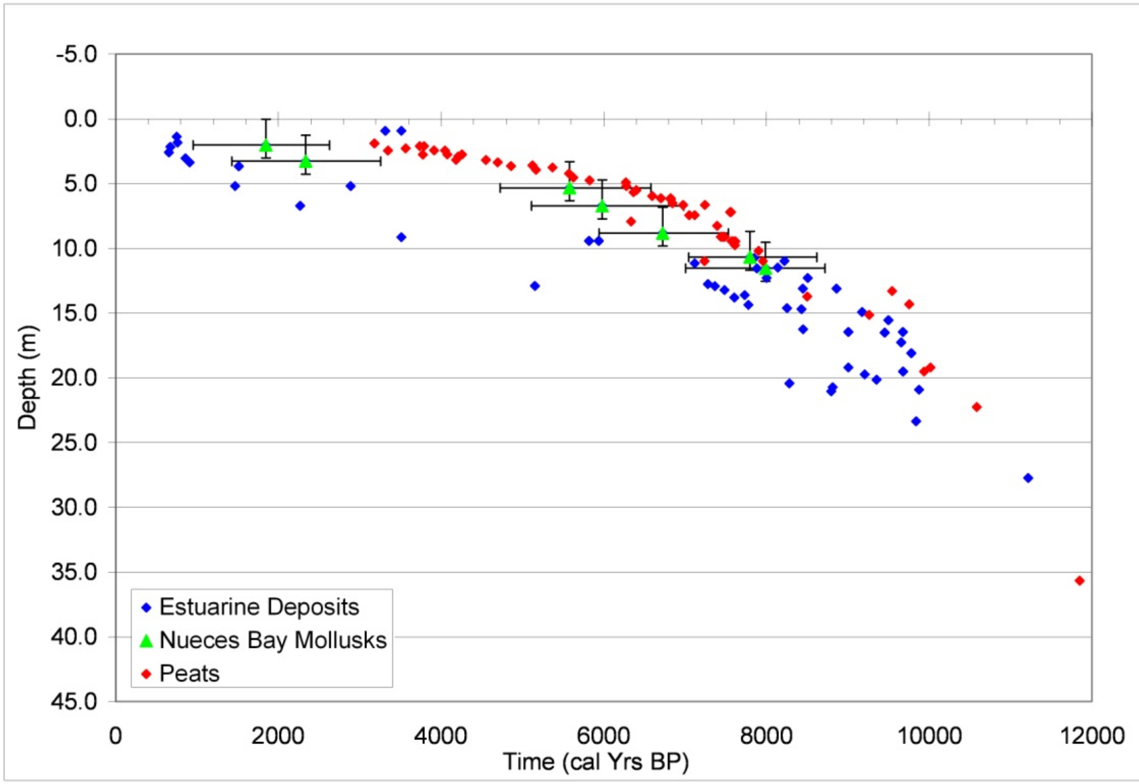


**Figure 3.** Sea-level indices from across the coastal area of the northwestern Gulf of Mexico. Data come from Shepard and Moore (1954), Curray (1960), Nelson (1970), Rodriguez et al (2004), Tornqvist et al.(2004) and Simms et al.(2008). Estuarine deposits were obtained from either wood fragments or mollusk shell. Peats were interpreted by each of the representing authors to represent basal peats. Nueces Bay dates were obtained from mollusk shells (Simms et al., 2008).

(Bryant and Holloway, 1985).   During the  *Late-middle Holocene* (6.0 to 5.0 ka.), the abundance of C4 plant biomass reached a maximum of 85 to 90%, indicating warmer and dryer climatic conditions with prairie expansion (Nordt et al., 1994).  By the *Early-Late Holocene* (4.0 ka.), Nordt et al.(1994) indicates that C4 plant biomass decreased to 65 to 75%, which is interpreted to represent a time of cooler and wetter climatic conditions. However, Toomey et al (1993) suggests that between 5.0 to 2.5 k.a. conditions were dryer than any other time in the last 20.0 k.y. on the Edward Plateau.  This is based on a complete disappearance of species  that thrived in wetter climates from the Hall's Cave faunal records (Toomey et al., 1993).  During the *Late Holocene* (2.5 to 1.0 k.a), mesic conditions were returning to the Edward Plateau.  The observations of Toomey et al (1993) indicate a return of small vertebrates requiring high moisture conditions.  Bryant and Holloway (1985) also found an increase in grass and pine pollen suggesting wetter conditions during this time period.  Data for interpreting the last 1.0 k.a on the Edward Plateau is very limited; however, Toomey et al. (1993) suggest a subtle change to more xeric conditions based on a shift in the Hall's Cave faunal record. Taxa from the last 1 ky are dominated by *Notiosorex,* which is adapted to drier conditions and persists in the area today.

# CHAPTER III

# METHODOLOGY

A combined geomorphological and sedimentological approach was used to reconstruct the depositional environments of Copano Bay. In addition, detailed grain-size analysis was used to reconstruct paleo wind energy. To study the depositional history and the impact of changing wind energy on the evolution of Copano Bay, we collected four rotary-push cores up to 16 m in length and two vibarcores up to 3 m in length aboard the *R/V Trinity.* The locations of the cores taken within Copano Bay are shown in Figure 4.

**Core Description:**

Sediment cores were split in two at the Oklahoma State University Sediment Laboratory. The archive halves were stored in a refrigerator and the sample halves were photographed and described for sediment texture, composition, color, structure and fauna. Color of the wet sediment samples were compared with a Munsell Soil Color chart. Canvas 9.1 was used to create lithostratigraphic columns of the cores. Grain-size analysis was conducted using laser diffractometry every 5 cm on core CB08-02 and every

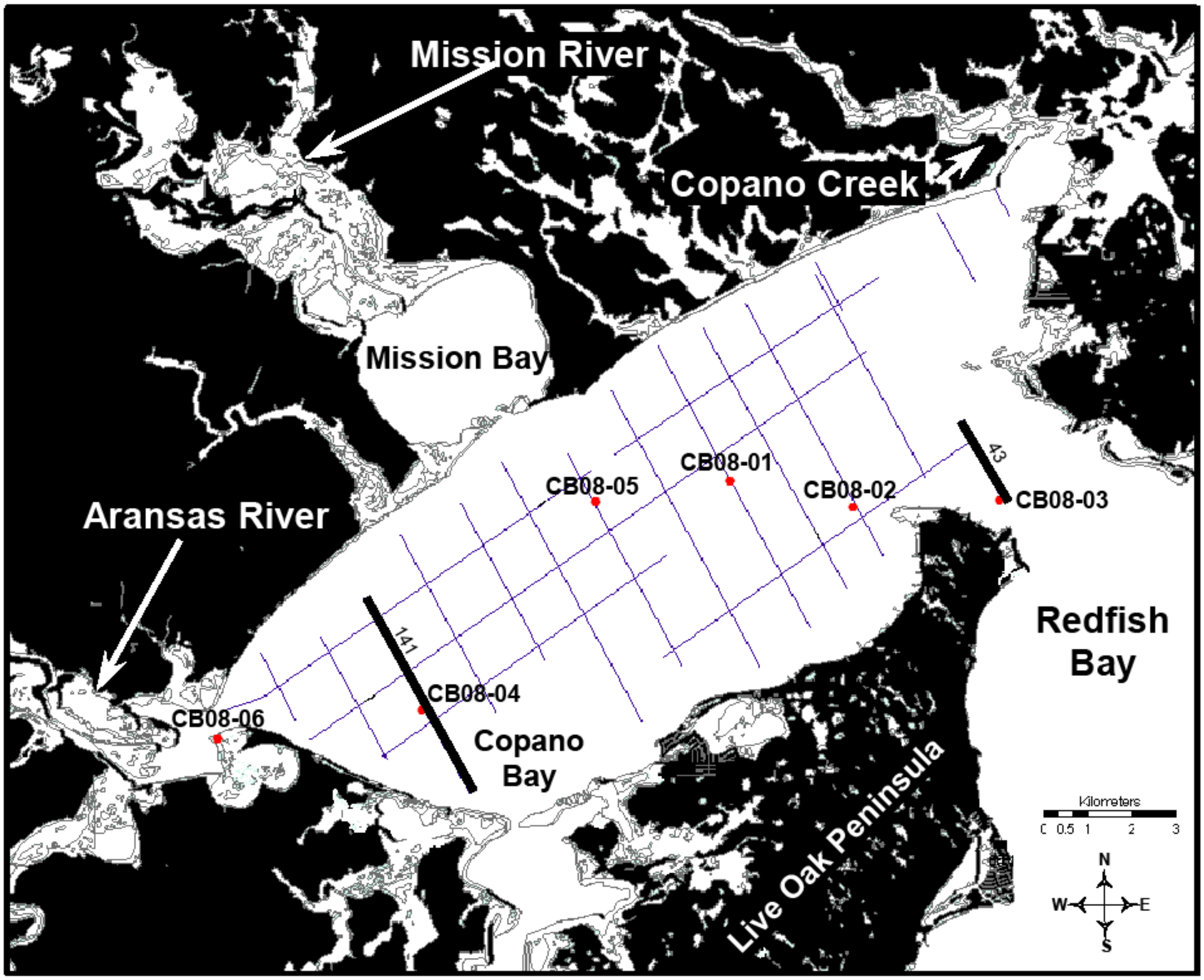


**Figure 4.** The location of seismic lines and cores within Copano Bay.

20 cm on all other cores. All sediment samples were chemically treated with 5 ml of 10% hydrogen peroxide and 10 ml of 10% hydrochloric acid to remove any organic and carbonate material.

The results of the grain-size analysis reflect the grain-size distribution of only the siliciclastic fraction of the sediment sample. After acid treatment sediment samples were soaked in 30 ml of a 5.5g/L solution of sodium metaphosphate for 24 hours to prohibit flocculation. All measurements were performed on a CILAS 1180 laser particle-size analyzer, which results in a grain size distribution with 99 size classes in the size range of 0.04-2500 µm. A refractive index of 1.544 was used following the 'pipette' method of Sperazza et al. (2004). Each measurement was repeated to test for bias during the pipette transfer of the sediments. The cores were described using coarse-fraction analysis modified from the procedures of Shepard and Moore (1954). Sedimentary structures, macofauna, as well as grain-size distribution curves were also documented and aided in the interpretation of depositional environments. X-rays were taken of selected core segments used to help identify sedimentary structures.

**Surface samples:**

The comparison of grain-size frequency curves (GSFC) from other bays along the northwetern Gulf of Mexico were examined to see if our findings in Copano Bay were consistent with other bays on the central Gulf Coast of Texas. Surface grab samples and/or surface samples from cores were used for the comparison of GSFC. Surface samples were obtained from Copano, Matagorda, Lavaca, Galveston, and Corpus Christi Bays (Figure 2).

Grain-size analysis was conducted with the CILAS 1180 with the same parameters and pretreatment as the other samples.

**Seismic Data:**

Dr. Tim Dellapenna and students at Texas A&M Galveston obtained over 200 2-D seismic survey lines with spacing intervals of 150 m in Copano Bay, TX. The seismic survey was limited to areas with a minimum water depth of 1.2 m. The CHIRP survey was conducted using an Edgetech® 216S Full Spectrum Subbottom CHIRP seismic sonar towfish and the Triton Elics Delph Seismic® software package. The seismic sonar operates on a range of 2–16 kHz to profile sedimentary strata. The CHIRP fish was suspended just below the surface of the water from a davit on the port side of the stern of the *R/V Sammy Ray*. The CHIRP data was used to identify any underlying geological features and provide a stratigraphic framework for the bay deposits. The location of seismic lines and cores are shown in Figure 4.

Seismic data was interpreted following the procedures defined by Mitchum et al. (1977). Based on previous seismic studies of the Pleistocene/Holocene sediments of the Gulf of Mexico (Wright, 1980; Maddox et al., 2008), an average velocity of 1500 m/s was used to convert time to depth.

**Chronostratigraphy:**

Radiocarbon Accelerator Mass Spectrometry (AMS) dates of mollusks were obtained to determine the age of major stratigraphic surfaces and to establish a chronostratigraphic framework for the deposits within Copano Bay. A total of 11 radiocarbon dates were obtained from mollusk shells from selected cores. Samples were dated at the University of

Tokyo, Japan and Rafter Radiocarbon Laboratory in New Zealand using AMS techniques. Whenever possible, articulated shells were selected for radiocarbon dating. In the absence of articulated shells, valve halves or gastropods were selected that did not show signs of abrasion, minimizing the probability of post-depositional transportation.

Radiocarbon ages are reported in years before present (cal yr BP) with two-sigma probabilities of the calibration. All radiocarbon program ages were calibrated using the Northern Hemisphere Marine curve of Calib 5.0.2, (September 2009 and November 2009), which accounts for atmospheric variation in radiocarbon over time and its interaction with the ocean by comparing sample dates against a calibrated data set (Stuiver and Reimer, 2005).

**Paleogeographic Map:**

Paleogeographic maps of the bay through time were constructed using Arc Map 9.2 based on seismic and sedimentary facies. These maps illustrate the timing and nature of valley fill within Copano Bay.

# CHAPTER IV

# RESULTS

## Sedimentology

The six cores from Copano Bay reached depths of 16 m (Figure 5). The cores contained a total of ten facies that can be grouped into four facies groups. The four facies groups identified within the Copano Bay cores include: mud facies, sand facies, oyster-reef facies, and oyster shell-hash facies (Figure 6). The mud facies is the most widespread facies and contains less than 20% sand. The sand facies consist of more than 20% sand with most facies containing 50% sand. The oyster shell-hash facies is associated with the oyster reef-facies. Figure 8 are photographs depicting some of the sedimentary facies.

### Mud Facies (MF):

MF1. Mud facies 1 is a dark gray structureless homogenous mud that typically consists of about 10% sand, 60% silt and 30% clay (Figure 7a). Shells and shell fragments are very sparse, but do contain a few specimens of *Nuculana concentria*, *Abra aequalis* and *Mercenaria campechienis texana.* This facies is present in the upper 2 m of cores taken within Copano Bay where oyster reefs are not present. This facies is interpreted to be middle-bay deposits analogous to the modern open-bay environment.

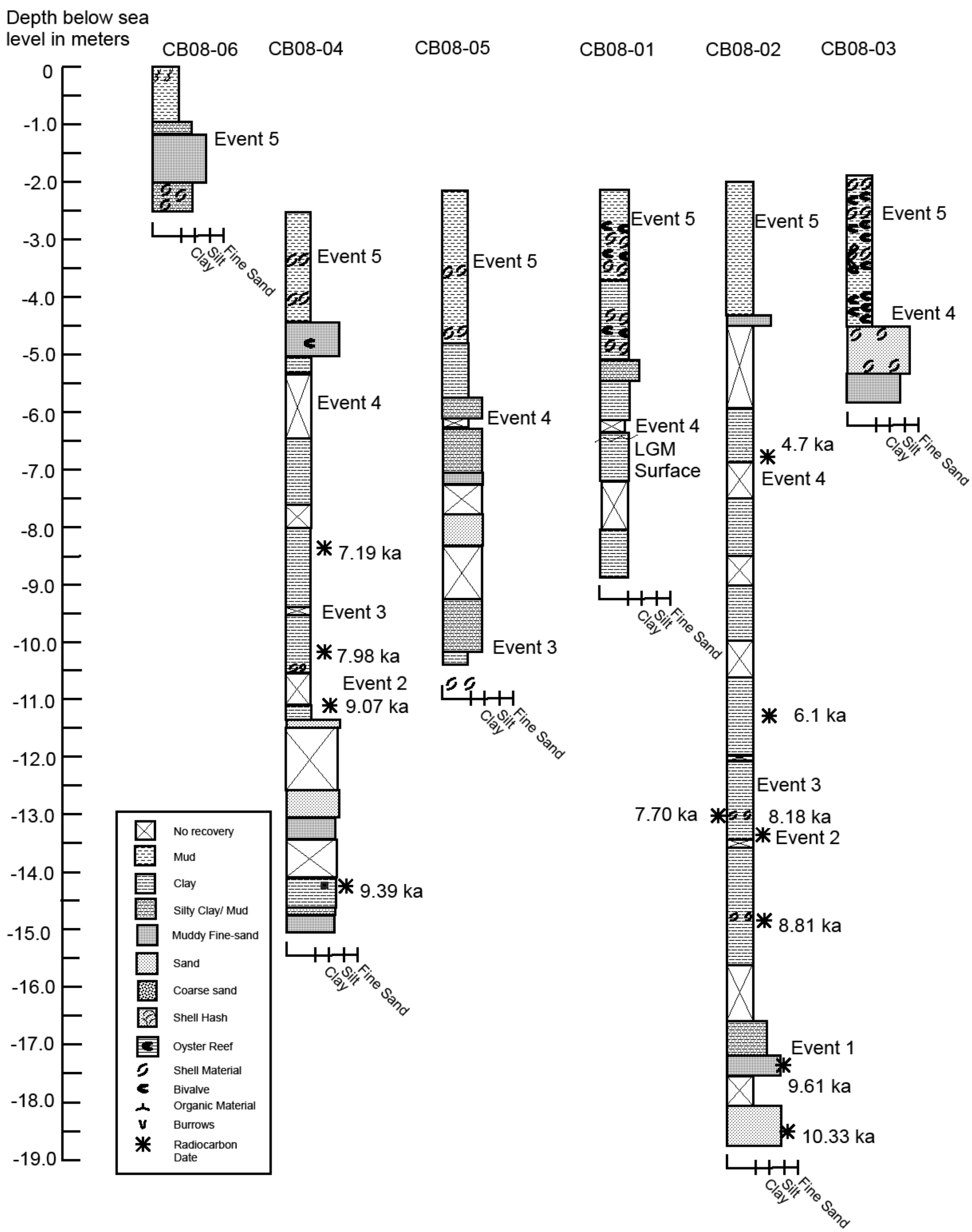


**Figure 5.** Core descriptions from Copano Bay with radiocarbon dates, see Figure 4 for locations.

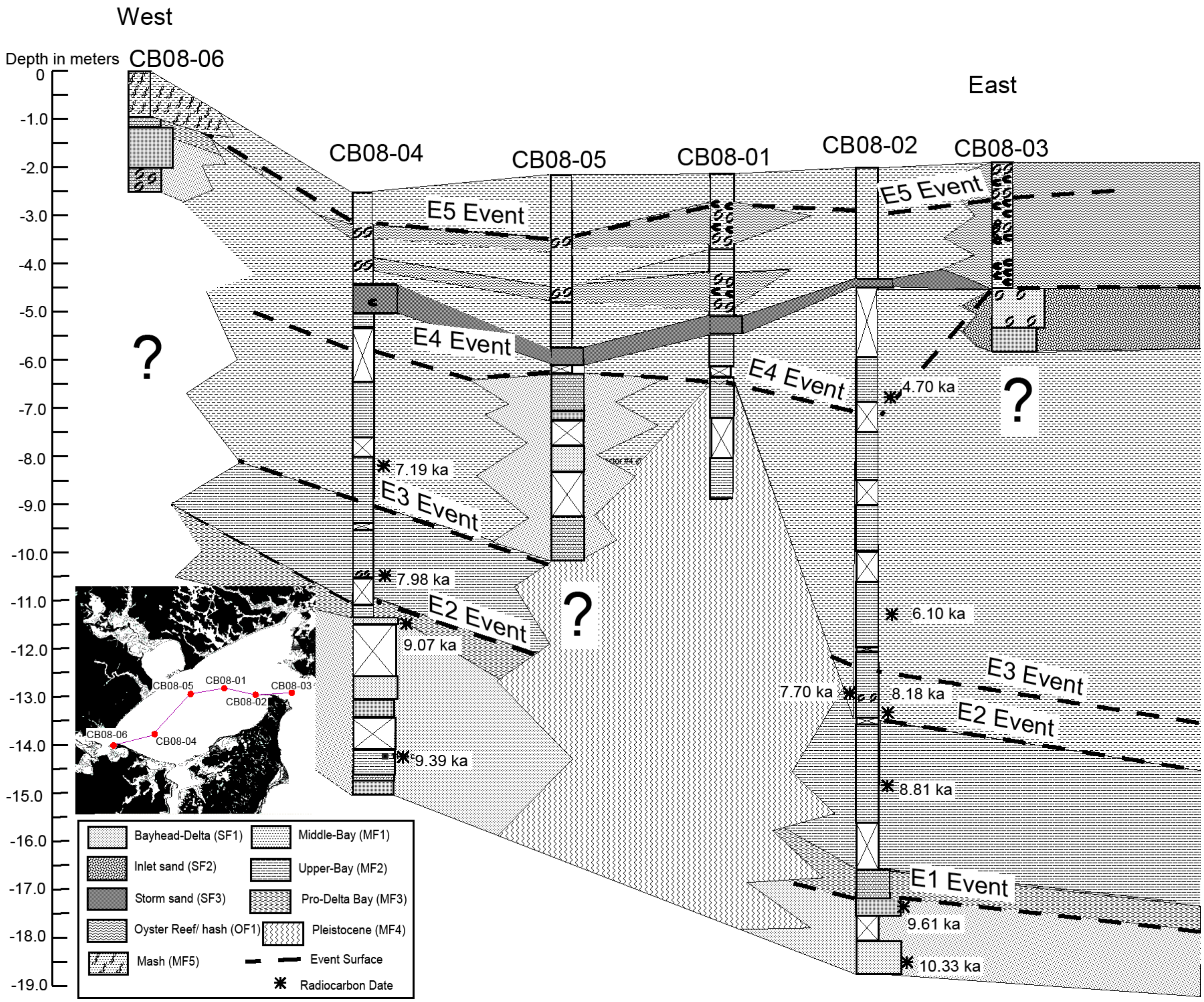


**Figure 6.** Facies diagram of Copano Bay.

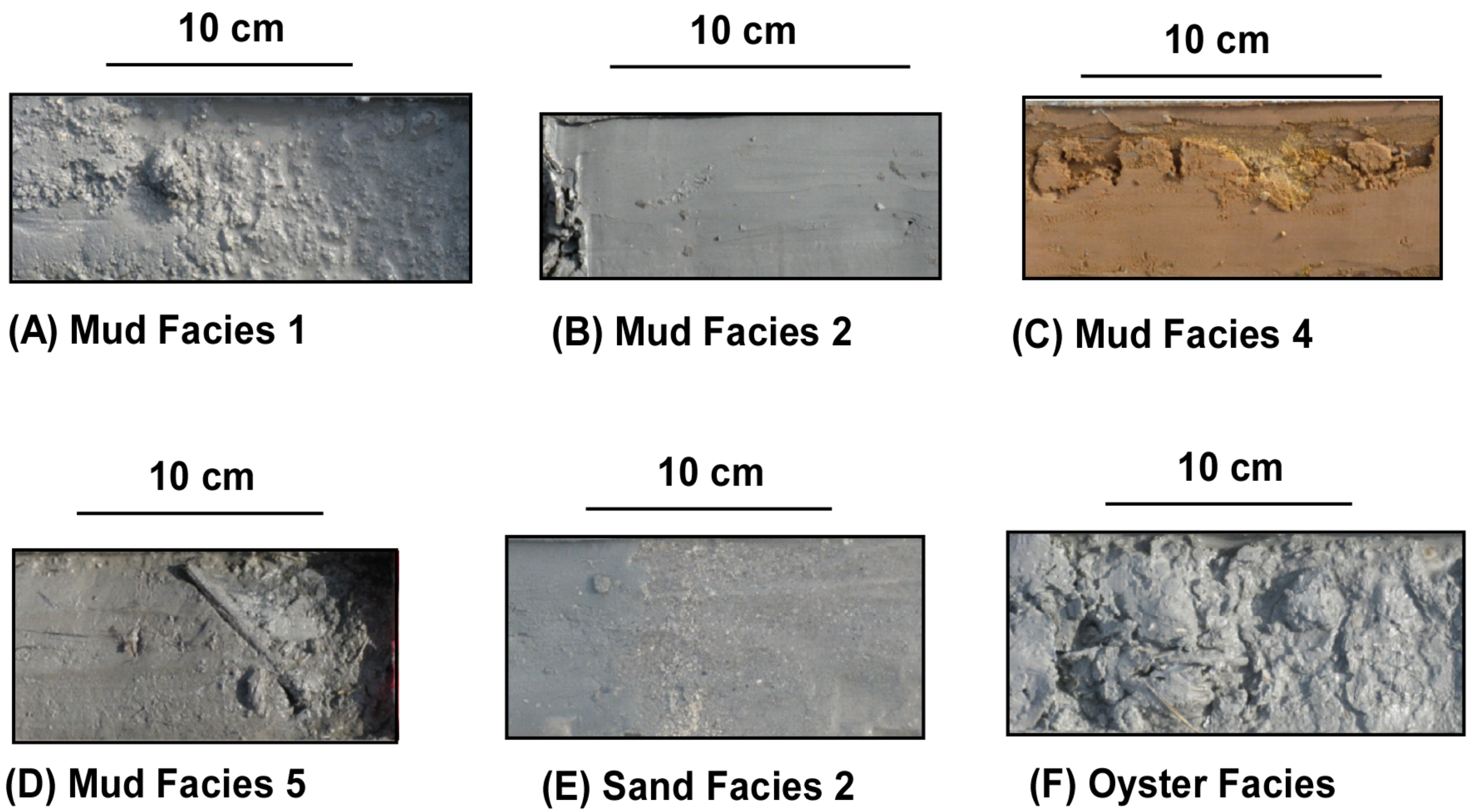


**Figure 7.** Photographs depicting some of the selected sedimentary facies. A) Mud Facies 1 from a depth of 0.15m in core CB08-01, B) Mud Facies 2 from a depth of 11.3m in core CB08-02, C) Mud Facies 4 from a depth of 6.2m in core CB08-01, D) Mud Facies 5 from a depth of 0.1m in core CB08-06, E) Sand Facies 2 from a depth of 3.5m in core CB08-03, F) Oyster Facies from a depth of 1.5m in core CB08-03.

MF2  Mud facies 2 is a gray structureless homogenous mud very similar to MF1 but lighter in color and better consolidated (Figure 7b).  MF2 typically consists of about 5% sand, 60% silt and 35% clay.  Lamina scale, sandy storm deposits of SF3 are found within MF2.  Shells and shell fragments found include specimens of *Nuculana concentria, Abra aequalis, Mercenaria campechienis texana, Rangia flexuosa and Mulinia lateralis.* This facies is interpreted to represent upper-bay deposits.

MF3.  Mud facies 3 is a dark gray structureless homogenous mud very similar to MF2 but sandier and darker in color.  It typically consists of about 10% sand, 65% silt and 25% clay.  Shells and shell fragments are very sparse, but do contain a few specimens of *Nuculana concentria* and *Rangia flexuosa.*  Plant material is also present.  This facies is interpreted to represent a prodelta environment.

MF4. Mud facies 4 is a red silty-clay encountered in the bottom part of core CB08-01 (Figure 7c).  It consists of 13% sand, 68% silt and 19% clay.  MF4 is a stiff dense red clay that is believed to be Pleistocene in age.

MF5. Mud facies 5 is a dark gray organic rich mud containing 9% sand, 78% silt and 12% clay (Figure 7d).  MF5 contains no shells, but contains several roots and plant fragments.  This facies is interpreted to represent marsh deposits and is only found in core CB08-06.

**Sand Facies (SF):**

SF1. Sand facies 1 is a gray organic-rich, homogenous, muddy very fine to fine sand. It typically contains about 50% sand, 34% silt, and 16% clay.  Shells and shell fragments are sparse, but occasionally *Rangia flexosa*, *Acteocina canaliculata* and *Bittium varium* are found.  No sedimentary structures are found. This facies is interpreted to be delta-plain deposits.

SF2. Sand facies 2 is a well sorted medium-grained sand (Figure 7e). SF2 consists of 75-95% sand.  Some oyster shell fragments are present.  This facies is interpreted to represent tidal-inlet deposits.

SF3. Sand facies 3 is a fine-grained homogeneous structureless sand incased in clay, and consists of about 20-55% sand, 30-50% silt, and 11-30% clay.  SF1 is sandier at its base and becomes more clay-rich towards the top.  Very few small shell fragments are present within this facies.   This facies is the sandy lamina found within MF2.  This facies is believed to represent storm deposits.

**Oyster Reef Facies (OF):**

OF1.  Oyster reef facies 1 consists of articulated and un-articulated oysters within a muddy silty matrix (Figure 7f).  Oysters are mostly *Crassostrea virginica* but some *Ostrea equestris* are present.

**Shell-hash Facies (ShF)**

ShF1.  This shell-hash facies is a structureless pooly sorted conglomerate of whole and fragmented oyster shells, mostly of *Crassostrea virginica.* ShF1 is found in association with the oyster reef facies (OF1), where it is the thickest near oyster reefs.  This facies is interpreted to represent oyster-reef debris and is found in association with oyster reef facies.

**Grain-Size Analysis:**

A total of three hundred and sixty two grain-size samples were examined in this study. Sediments included in the grain-size analysis were from the six cores and forty surface samples from Copano, Matagorda, Lavaca, Galveston, and Corpus Christi Bays. Each grain-size analysis yielded a grain-size frequency curve (GSFC). Fluvial and deltaic sediments were found to be unimodal and the mode typically ranged in size between 70-125 μm (Figure 8). Upper-bay sediments were found to be polymodal usually consisting of 4-5 modes (Figure 8). Upper-bay sediment modes typically ranged in size between 1-100 μm (Figure 8). Middle-bay sediments were found to be polymodal usually consisting of 3-4 modes (Figure 8). Middle-bay sediment modes typically ranged in size between 1-50 μm (Figure 8). Tidal-inlet sediments were found to be unimodal and the mode ranged in size between 130-170 μm (Figure 8).

**Seismic:**

A total of one hundred and twenty three km of 2-D seismic lines were used in this study. Five seismic facies are indentified above the Last Glacial Maximum unconformity (Figures 9 and 10). Seismic facies were distinguished based on seismic properties. Seismic facies are correlated to sedimentary facies found within the six cores.

**Seismic Facies (F):**

F1. Seismic facies 1 is composed of medium amplitude, chaotic reflections with some very discontinuous sigmoid-oblique reflections (Figure 9 and 10). In terms of sedimentology, seismic facies 1 corresponds with sedimentary facies SF1 and is interpreted to represent deltaic deposits.

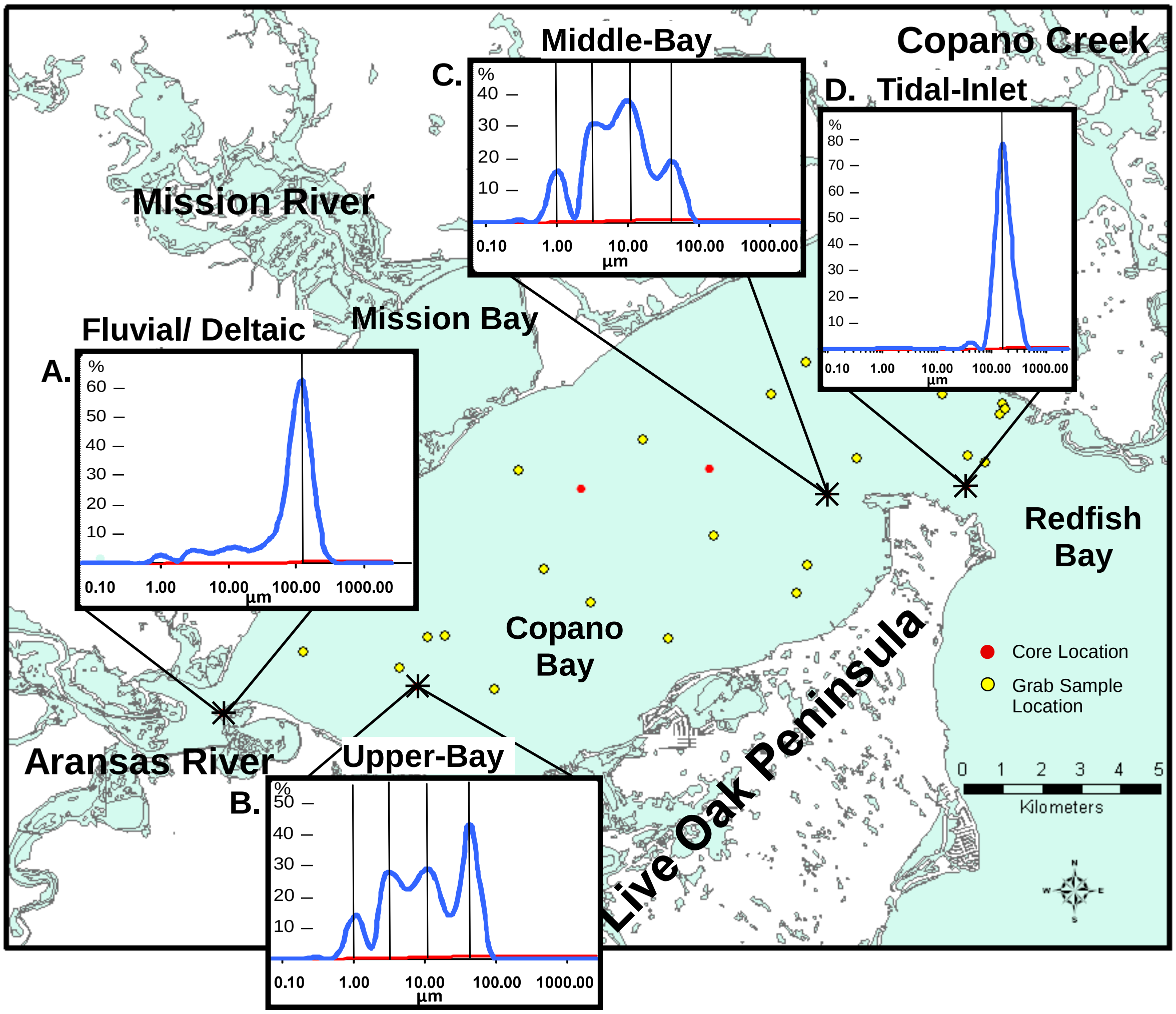


**Figure 8.** Map of Copano Bay showing location of all surface and core sediments samples with grain-size data. Also shown are four grain-size frequency curves from major environments found within Copano Bay: A) deltaic, B) upper-bay, C) middle-bay, and D) tidal-inlet.

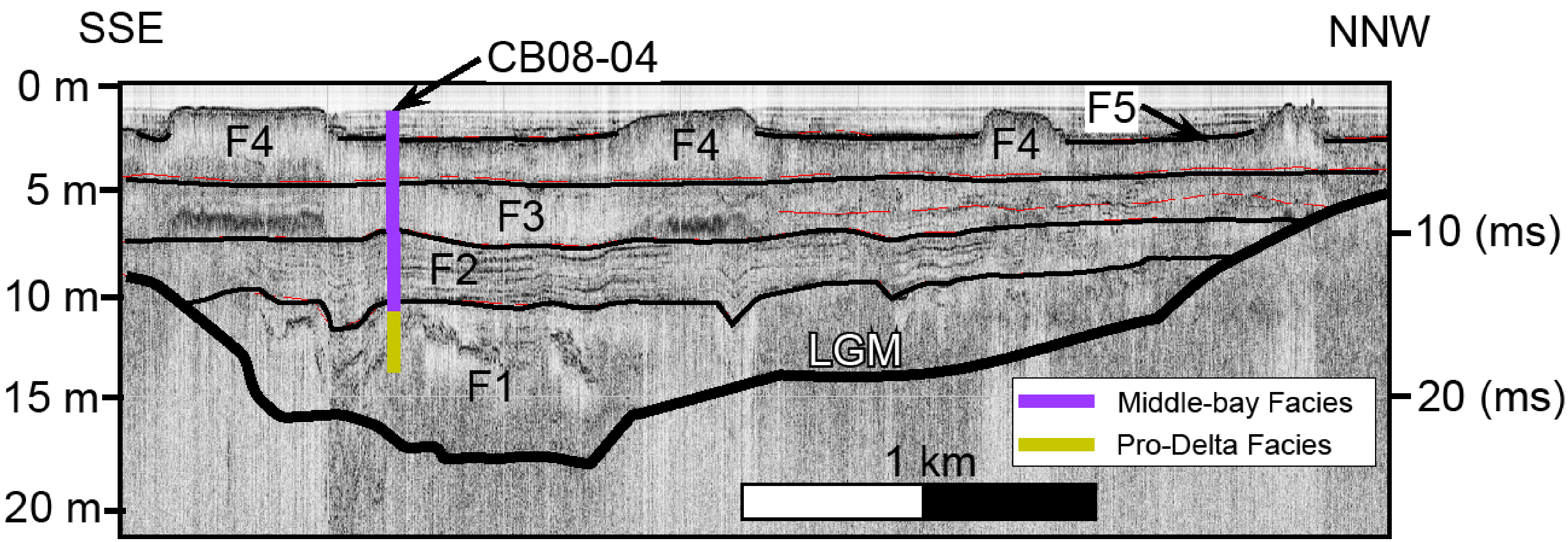


**Figure 9.** Seismic line 141 showing seismic facies F1-F5, parasequence boundaries separating seismic facies, the location of CB08-04 and the Last Glacial Maximum unconformity. See Figure 4 for seismic line location.

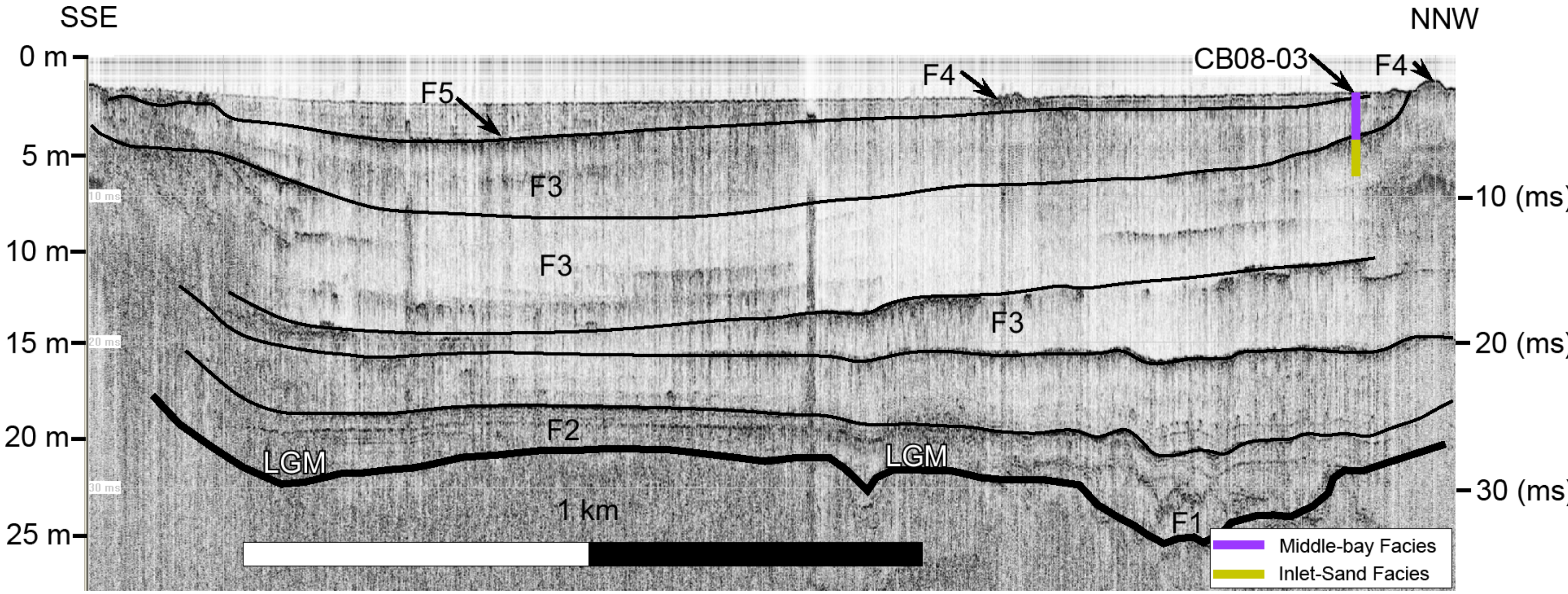


**Figure 10.** Seismic line 43 showing seismic facies F1-F5, the location of CB08-03, and the Last Glacial Maximum unconformity. Marked punctuations in seismic facies represent tidal revienment surfaces. See Figure 4 for seismic line location.

F2. Seismic facies 2 is a series of high amplitude nearly continuous parallel reflections (Figure 9 and 10). Cores that sampled F2 contain sedimentary facies MF1 and MF2. This seismic facies is interpreted to represent prodelta and upper-bay deposits.

F3. Seismic facies 3 is composed of low amplitude to nearly acoustically transparent reflections (Figure 9 and 10). Faint, sometimes wavy, continuous, parallel reflections are present. One or two high amplitude reflections are found within F3. These high-amplitude reflections are believed to represent sandy storm deposits. These hard reflections correlate to SF3. Cores that sampled F3 contain sedimentary facies MF1, MF2 and SF3. This seismic facies is interpreted to represent open-bay deposits.

F4. Seismic facies 4 is composed of mounded, high amplitude continuous, parallel reflections (Figure 9). This seismic facies is interpreted to represent oyster reefs.

F5. Seismic facies 5 is composed of high amplitude, continuous and parallel reflections (Figure 9). F5 almost always onlaps F4 (Figure 9). In terms of sedimentology, seismic facies 5 corresponds to sedimentary facies ShF1. In seismic profiles, this unit is associated with the oyster reef facies F4 (Figures 9 and 10).

**Events:**

Five parasequence boundaries are observed in both seismic and core data (Figures 5, 6, 9 and 10). These five parasequence boundaries mark changes in seismic and/ or sedimentary facies. Identified parasequence boundaries are referred to as events and are numbered sequentially (E1-E5) starting above the Last Glacial Maximum unconformity and continuing upwards.

**Last Glacial Maximum Unconformity Structure Map:**

Seismic data was also used to map the incised valleys of the Mission, Aransas, and Copano rivers, which were flooded to form Copano Bay (Figure 11)   The map was created with the use of six sediment cores and nineteen 2-D seismic survey lines.  The geomorphology of the valley had an important impact in the flooding history of the bay. Copano’s paleo-valley is similar to the other incised valleys on the Texas Gulf coast in that it has a deep and narrow incision near the center of the valley.

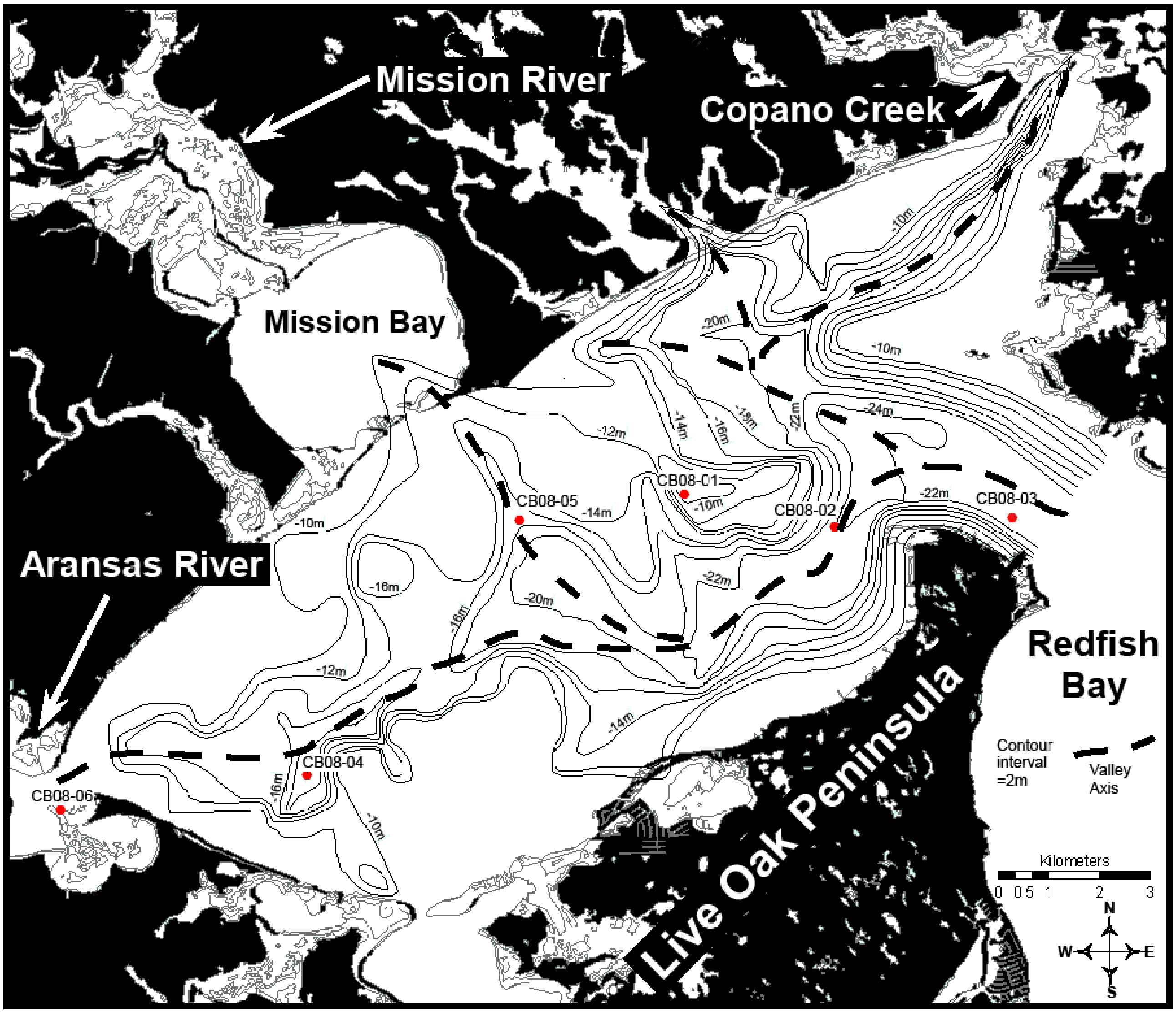


**Figure 11.** Topography of the Last Glacial Maximum unconformity beneath Copano Bay obtained from the interpretation of seismic and core data from this study. Contour interval is 2 m. Valley axes are shown as dashed lines.

**Radiocarbon Dates:**

A total of 11 radiocarbon dates were obtained from shells to establish a chronostratigraphic frame work for Copano Bay (Table 1). Whenever possible, articulated shells were selected for radiocarbon dating. All radiocarbon dates are reported as years before present (cal yr BP). All radiocarbon dates taken from cores within Copano Bay fall in stratigraphic order.

**Table 1.** Radiocarbon dates collected for this study

| Core | Sample depth in core (m) | Description/Species | Lab | Lab Code | δ¹³C | Conventional ¹⁴ C Corrected for δ¹³C (yr B.P.) | Calibrated (2 δ ) range (Cal yr B.P.) | Calibrated mean age (Cal yr B.P.) |
|---|---|---|---|---|---|---|---|---|
| CB08-02 | -4.7 | articulated *Nuculana Concentrica* | University of Tokyo | MTC-13317 | -0.33* | 4510±50 | 4560-4830 | 4700 |
| CB08-02 | -9.2 | valve *Nuculana Concentrica* | University of Tokyo | MTC-13318 | -0.33* | 5740±45 | 6010-6260 | 6140 |
| CB08-02 | -10.9 | articulated *Nuculana Concentrica* | University of Tokyo | MTC-13319 | -0.33* | 7241±90 | 7560-7910 | 7735 |
| CB08-02 | -11.2 | articulated *Nuculana Concentrica* | University of Tokyo | MTC-13320 | -0.33* | 7720±55 | 8040-8320 | 8180 |
| CB08-02 | -13.1 | articulated *Nuculana Concentrica* | Rafter GNS Science | NZA-32347 | 0.60 | 8264±50 | 8660-8970 | 8815 |
| CB08-02 | -15.3 | articulated *Rangia Flexuosa* (Juvenile) | University of Tokyo | MTC-13123 | -0.33* | 8891±120 | 9285- 9935 | 9610 |
| CB08-02 | -16.6 | valve *Rangia Flexuosa* (Juvenile) | University of Tokyo | MTC-13124 | -0.33* | 9458±65 | 10180-10480 | 10330 |
| CB08-04 | -4.9 | articulated *Nuculana Concentrica* | Rafter GNS Science | NZA-32348 | 0.60 | 6654±45 | 7060-7290 | 7190 |
| CB08-04 | -7.7 | articulated *Rangia Flexuosa* | Rafter GNS Science | NZA-32302 | 0.50 | 7525±40 | 7910-8110 | 7980 |
| CB08-04 | -8.9 | valve *Rangia Flexuosa* | Rafter GNS Science | NZA-32346 | -1.10 | 8453±50 | 8960-9240 | 9070 |
| CB08-04 | -11.7 | *Turbonilla* | Rafter GNS Science | NZA-32345 | -1.80 | 8713±50 | 9270-9490 | 9390 |

* Average δ¹³ from *Nuculana Concentrica* from the central Texas coast

# CHAPTER V

# DISCUSSION

## **Bay Evolution:**

The overall succession of Holocene sediments and seismic facies beneath Copano Bay illustrates a classic transgression (Figure 6). The vertical succession of sediments can be subdivided by parasequence boundaries or events (E1-E5). These events are interpreted to be either flooding surfaces or other gradual environmental changes. Flooding surfaces are interpreted as periods of rapid change within the estuary resulting in back-stepping events marked by sharp contacts between basin-ward sediments above and more landward sediments below the surface (Anderson et al., 2001). Simms et al. (2008) suggest that flooding surfaces within Corpus Christi Bay form in as little as 200 yr. Five events (E1-E5) or parasequence boundaries are evident within the Holocene sediments of Copano Bay. Both seismic and core data were used to identify these events within the bay sediments. Where good constraints exist within Copano Bay, e.g. event 2, the surfaces also appear ro have formed in as little as 200 years. Palegeographic maps were constructed based on the seismic and sedimentary facies found between events (Figure 12a-e).

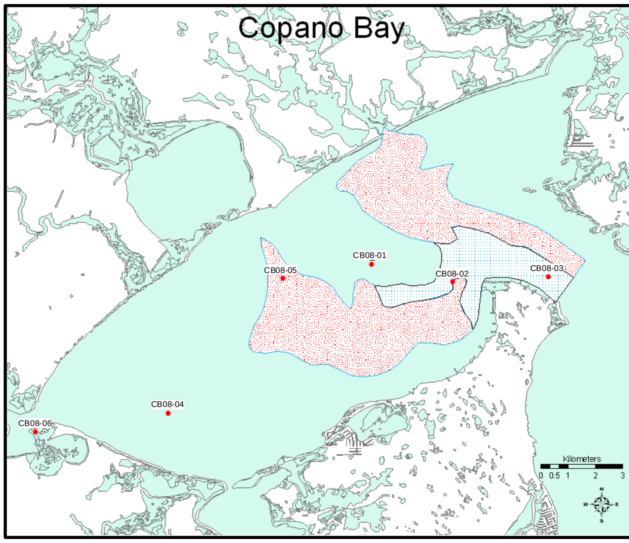


(A) 9.6-8.2 ka

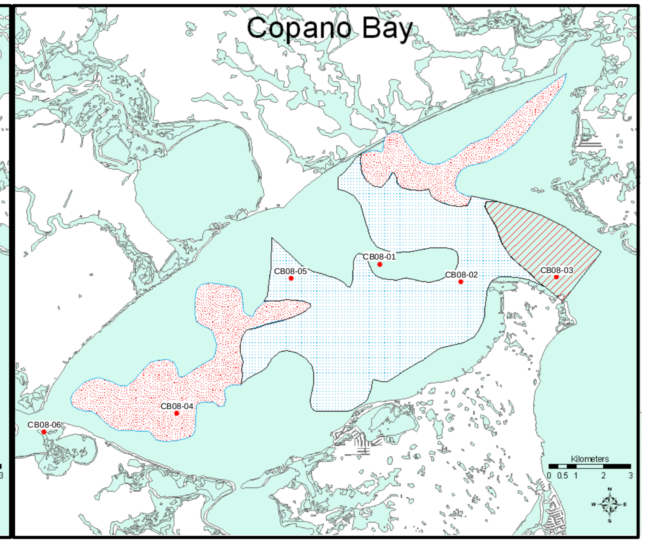


(B) 8.2-7.5 ka

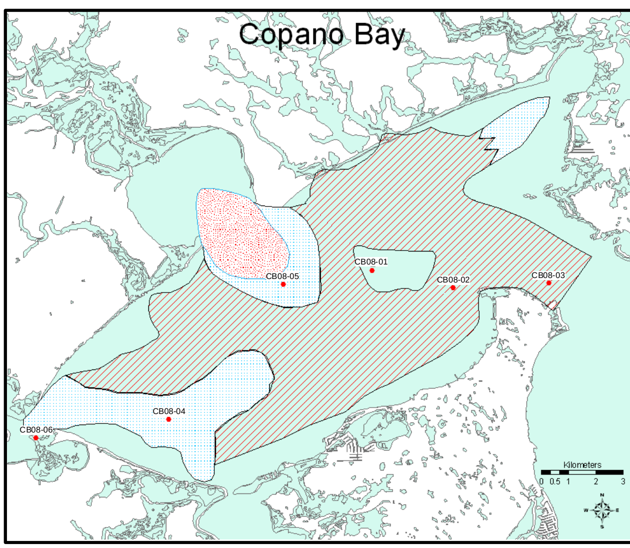


(C) 7.5-4.8 ka

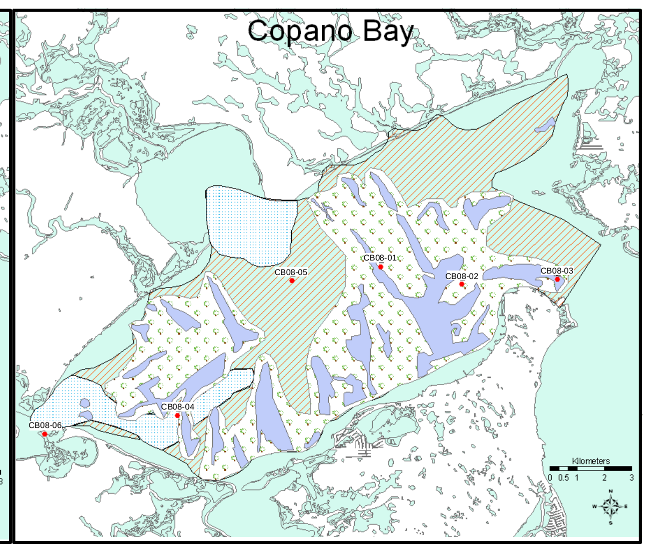


(D) 4.8-2.5 ka

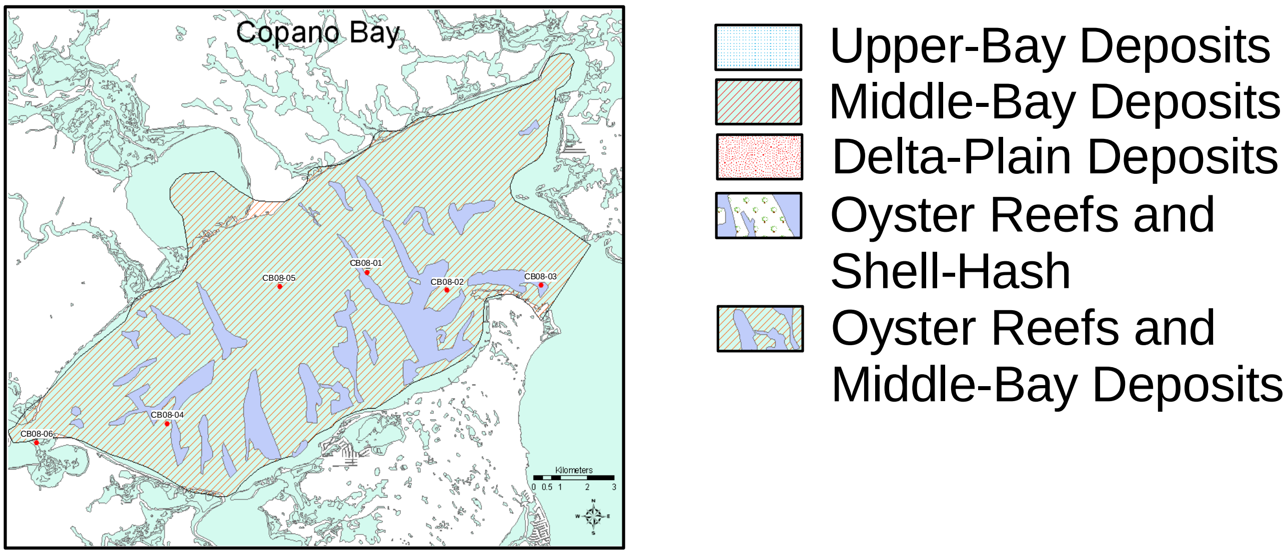


(E) 2.5 ka-present

**Figure 12.** Paleogeography of Copano Bay illustrating environmental changes that occurred between each event. (A) Paleogeography prior to E2 (8.2 ka), (B) Paleogeography after E2 but prior to E3 (8.2-7.5 ka), (C) Paleogeography after E3 but prior to E4 (7.5-4.8 ka), (D) Paleogeography after E4 but prior to E5 (4.8-2.5 ka), (E) Paleogeography after E5 (2.5 ka).

**Event 1 (E1)**

Event 1 represents the initial flooding and marks the first encroachment of estuarine environments within Copano Bay. The oldest facies examined within Copano Bay lies between E1 and the LGM. Only one core, CB08-02, samples Holocene below E1 at a depth of -14.5 m. Seismic facies below E1 and above the LGM are interpreted to represent delta plain or distributary channel deposits (Figure 12a). Estimations based on sedimentation rates from radiocarbon ages constrain the timing of E1 to around 9.6 ka. At the scale of the seismic data, terminations are not observed above and below the surface. This suggests that the seismic reflection does not represent a hiatus, but likely a time line. Other bays on the Texas Gulf Coast underwent initial flooding around the same time as Copano Bay (Anderson et al., 2008; Maddox et al., 2008; Simms et al., 2008).

**Event 2 (E2)**

Event 2 is marked by a flooding surface. Above the flooding surface the estuarine environments back-stepped landward approximately 7.5 km resulting in a large increase in the size of the bay (Figure 12b). A large portion of the bay experienced a change from a deltaic to an upper-bay environment (Figure 12b). The timing of this flooding event is estimated to have occurred about 8.2 ka, based on sedimentation rates from radiocarbon ages in cores CB08-02 and CB08-04 (Table 1).

Two cores sampled this interval: CB08-02 and CB08-04. In CB08-04, the unit above and below the 8.2 ka event is composed of fluvial and deltaic deposits. The 8.2 ka flooding event in CB08-02 is found at -11.2 m. In CB08-02, deposits above the 8.2 ka event are middle-bay deposits and deposits below the 8.2 ka event are upper-bay deposits.

A major climatic event is documented to have occurred at 8.2 ka. The cause of this event is thought to have been the release of meltwater into the North Atlantic Ocean due to the draining of Lake Agassiz-Ojibway during the final breakup of the Laurentide ice sheet (Barber et al., 1999; Clark et al., 2001; Thomas et al., 2007). Tornqvist et al (2004) originally suggested that sea level rose around 1.2 m during the 8.2 ka climatic event as a result of the additional meltwater from the Laurentide ice sheet. However, more recently, Kendall et al (2008) revisits the problem using glacio-hydro-isostatic models and suggested that sea level only rose around 0.4 m in the Gulf of Mexico as a result of the draining of Lake Agassiz-Ojibway during 8.2 ka. E2 is interpreted to be the result of this rapid sea-level rise event. A similar event has been documented in other coastal system worldwide (Cronin et al., 2007; Hori and Saito, 2007)

**Event (E3)**

Event 3 is interpreted as a flooding surface that is manifested in most cores by middle-bay deposits resting on upper-bay deposits (Figure 12c). However, in core CB08-05 fluvial and delta plain-deposits of the Mission River are found between -8.0m and -3.5m and E3 passes through the middle of these deposits. Above E3 the Mission River delta progrades past the location of core CB08-05 (Figure 12c). Core CB08-04 encounters E3 at -8.4 m and is manifested by middle-bay sediments resting on upper-bay sediments. Based on radiocarbon ages in core CB08-04 and CB08-02, E3 formed around 7.5 ka. E3 marks the final stages of the flooding of the deep, narrow parts of the valley. E3 occurred at the same time as a proposed episode of rapid (18 mm/yr.) sea-level rise (Yu et al., 2007; Milliken et al., 2008a). Thus, E3 is interpreted to be the result of this global event.

**Event 4 (E4)**

E4 is interpreted as a flooding surface. E4 is manifested in most cores by middle-bay deposits and oyster shell-hash deposits above and below the flooding surfaces throughout much of the bay. E4 is estimated to have formed around 4.8 ka based on radiocarbon ages in core CB08-04 and CB08-02. After 6.0 ka the rate of sea-level rise within the Gulf of Mexico decreased considerably to around 1.4 mm/yr and by 4.0 ka, sea-level slowed to 0.4-0.6 mm/yr. (Simms et al., 2007; Milliken et al., 2008a). The recognition of flooding events is less pronounced after 6.0 ka. The ice sheet models of Huybrechts (2002) and Lambeck et al. (2002) show that by 6.0 ka most of the ice sheets had disappeared and no known rapid increases in the rate of sea level are known. Thus any flooding events after this time period are most likely the result of other mechanisms such as changes in sediment supply to the bay or winds. Both of which may be a result of changing climate. Toomey et al (1993) and Nordt et al (1994) suggest that 5.0 to 2.5 ka were the driest conditions experienced on the Edwards Plateau of central Texas and adjoining areas during the Holocene. The drier conditions would have a twofold effect on Copano Bay. At the beginning of the dry period, the remaining root network of trees and shrubs would have kept the soil in place within the drainage basin while the decreasing effective moisture diminished. This process would have decreased the amount of sediment delivered to the bay. Prominent middle-bay deposits throughout the bay and a reduction in the size of the bay-head delta suggest that sediment delivered to the bay was diminishing. A diminishing sediment supply would also result in more clarity in the water column allowing oyster reefs to flourish (Foster-Smith, 1975). Oyster reefs are seen both in seismic profiles and in cores and are present through most of the bay today (Figure 12d). E4 is believed to have formed due to a deficiency in sediment supplied to the bay.  The flooding of the delta from the Mission River that formed during E3 is also consistent with a decrease in sediment supply (Figure 12d).

**Event 5 (E5)**

E5 is interpreted to represent an environmental change.  By this time the bay had evolved close to its current configuration (Figure 12e).  The unit above E4 is middle-bay deposits above oyster reefs.  E5 is estimated to have formed around 2.5 ka based on radiocarbon dates in core CB08-04.  E5 is interpreted as the onset or beginning of an increase in sediment delivered to the bay.  The timing of this sediment pulse is estimated to have occurred around 2.5 ka.  One effect of the dry period between 5.0 to 2.5 ka was a large increase in sediment input to the bay following a period of sediment deficiency.  This was the result of stripping of the upland soils on the Edwards Plateau and surrounding areas (Toomey et al., 1993).  By this time the bay had evolved close to its current configuration (Figure 12e).  The increase in sedimentation after 2.5 ka is thought to be the result of a climate change from drier conditions to wetter conditions within the drainage basins of Copano Bay.  The E5 sediment pulse is seen in seismic profiles but is not considered a flooding event in this study due to a lack of back stepping environments.

**Grain Size Modes:**

Estuaries are complex systems in which environmental conditions are impacted by marine, eolian and fluvial processes (Allen, 1971; Shideler, 1984).  Because of the complex nature of sediment sources to estuaries, the sediment grain-size distribution is polymodal (Kovacs, 2008).  Each mode of the GSFC represents a distinct transportation and or depositional mechanism (Pichevin, 2005; Kovacs, 2008).  Identifying and determining each mode of the GSFC is a crucial step for understanding and interpreting past environmental conditions within estuaries. Within Copano Bay 3 to 4 modes were found within the GSFC from core and surface samples of middle-bay sediments (Figure 13). Variations do exist with both the value and magnitude of the mode within each mode classification. These variations are thought to represent past environmental changes. All modes are discussed with relationship to middle-bay deposits.

**Modes 1 and 2 (M1-M2)**

Modes 1 and 2 are centered on 1 and 3 μm respectively and are found in almost all middle-bay deposits (Figure 13). The major sources and/or transportation mechanisms operating in Copano Bay may include suspended fluvial load, fluvial bed load, eolian dust, storm deposits, bay resuspension and suspended marine load. Copano Bay may be classified as a salt-wedge estuary; in such systems, deposition is dominated by suspended fluvial material and not suspended marine sediments, which are effectively blocked from entering the estuary (Brown et al., 1989). M1 and M2 are too small to have originated from an eolian source according to Stuut (2005) and Holz (2007) who suggest eolian deposits within marine sediments range in size from 8-48 μm. M1 and M2 are also too fine to represent fluvial bedload deposits. Thus, sediments within modes M1 and M2 are thought to originate as terrigenous clay delivered to Copano Bay by one or all of the rivers and or creeks flowing into the bay.

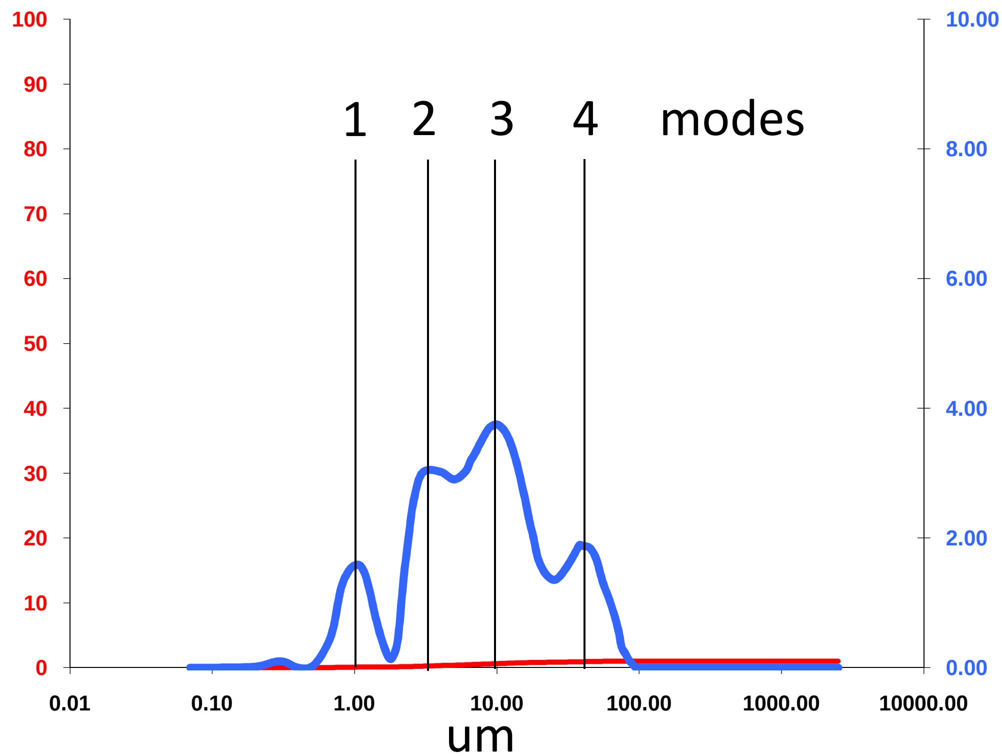


**Figure 13.** A typical grain-size frequency curve (GSFC) for middle-bay sediments within Copano Bay. The GSFC shown is from CB08-02 at a depth of -130 cm. This GSFC has four modes that are shown in microns (μm).

**Mode 3 (M3)**

Mode 3 is centered on 10 μm (Figure 13) but varies between 8.5 to 11 μm within Copano bay. The source of M3 could be either eolian dust or fluvial suspended load. The size of M3 falls between 8-48 μm and the findings of Stuut (2005) and Holz (2007) suggest that eolian deposits in marine sediments range in size from 8-48 μm. M3 is thought to have originated from an eolian dust source either delivered to the bay directly or delivered to the rivers and then delivered to the bay.

**Mode 4 (M4)**

Mode 4 is centered on 38 μm (Figure 13) but is highly variable throughout the data set and is not present in all middle-bay deposits. 38 μm is in the size range of eolian sediments (Stuut et al., 2005; Holz et al., 2007). M4 probably represents suspended silt or eolian deposits during times of very high wind velocity; velocities that are obtained during storms. M4 is thought to be of eolian origin and will not be dealt with in trying to determine paleo-wind strength in this study but will be used to determine storm frequency.

**Reconstructing Paleo-Winds:**

For the purpose of reconstructing paleo-wind energy for Copano Bay, the focus will be on modes 2 and 3, centered on 3 and 10 μm respectively (Figure 13). Changes in the ratio between the magnitude of modes 2 and 3 are thought to reflect variations in paleo-wind energy. Shideler (1984) has shown in Corpus Christi Bay that wind generated waves have the ability to re-suspend surface sediments in the particle size range of 2.5 to 6 μm. Based on Stokes's law, a 3 μm silica particle has a settling velocity of 14 cm/hr or 1 meter in 6.45 hours in tranquil brackish water. This low settling velocity would allow Copano Bay ebb tides to export the wind re-suspended material in the size range of 2.5 to 6 μm. This process would winnow the bay of sediment in the size range of 2.5 to 6 μm and would have a direct reduction on the magnitude of mode 2, centered at 3 μm.

Mode 3 (centered on 10 μm) is thought to be of eolian origin, so an increase in the magnitude of this mode would represent an increase of material transported to the bay by winds, most likely caused by increased wind activity. As no conservative mode was found in our GSFC, all paleo-wind energy will be reported as relative. A time of relatively high wind energy during the geological past would be represented in estuarine deposits by a large fraction of sediments centered on the 10 μm mode and a small fraction centered on the 3 μm mode.

Also in this study surface samples from Galveston, Corpus Christi, Matagorda, and Lavaca Bay were examined. The modes identified in Copano Bay are also present in most of these other bays. The placement of the modes varies slightly from bay to bay, but modes 1, 2 and 3 were within 2 μm of each other (Table 2). This further supports the assumption that each mode represents a distinct transportation and/or depositional mechanism operating in the estuaries along the central Texas Gulf Coast. However, more variation within the values of the modes existed within each bay than variation found from bay to bay (Table 2).

**Grain Size Trends:**

CB08-02 was chosen for detailed grain-size analysis with measurements taken every 5 cm. CB08-02 was chosen for detailed grain-size analysis because it contained the longest record of middle-bay deposits. The main objective of the grain-size analysis was to see if winds played a role in the sedimentation recorded in the bay. The best record of paleo-winds

**Table 2.** Grain-size modes from middle-bay deposits of Galveston, Corpus Christi, Matagorda, and Lavaca Bay.

| Bay Name | Number of Samples | Range of Mode 1 | Range of Mode 2 | Range of Mode 3 | Range of Mode 4 | Range of Mode 5 | Depth of Bay (m) | Fetch of Bay (km) |
|---|---|---|---|---|---|---|---|---|
| Copano | 33 | 1µm | 3µm | 8.5-11µm | 38-80µm | 93-160µm | 2.1 | 9.2 |
| Galveston | 1 | 1µm | 3µm | 12µm | 56µm | N.F. | 3 | 17.7 |
| Corpus Christi | 4 | 1µm | N.F. | 10-12µm | 36-90µm | N.F. | 3.9 | 19.8 |
| Matagorda | 1 | 1µm | 4µm | 13 µm | N.F. | 130µm | N.A. | N.A. |
| Lavaca | 1 | 1µm | 3µm | 11µm | 85µm | N.F. | 1.7 | 7.2 |

N.A. Not Applicable

N.F. Not Found

will be found in the part of the bay that is most affected by winds and has the best opportunity to preserve a record of paleo-wind energy. Wind would have the most influence on middle-bay deposits because the deltaic and upper-bay deposits are influenced dominantly by fluvial processes. Also middle-bay deposits are less affected by tides. Middle-bay grain-size data was interpreted based on the moment mean grain size (Figure 14b) and the ratio between the magnitude of modes 2 and 3 (Figure 14c).

In CB08-02, middle bay deposits are encountered at -11.2 m, immediately above the FS2 or the 8.2 ka flooding event. Figures 14a and b illustrate a red arrow representing a first order increase in the ratio between the magnitude of modes 2 and 3. This is thought to reflect an increase in the fetch as the bay widened during the overall transgression from 9.6 ka to the present (Figure 12a). The blue arrow represents a second order higher frequency curve and suggests variable wind energy. Figure 14b shows a gradual increase in the moment mean moving up the core (coarsing upward) which is thought to be a result of wind energy winnowing the bay of finer sediment. It should be noted that the moment mean size trend mimics the ratio between the magnitudes of M1 and M2, suggesting a correlation between moment mean and the ratio between the magnitude of modes 2 and 3. The ratio between the magnitudes of mode 2 and 3 is better than the moment mean grain-size at revealing paleo-wind energy as it not biased by storm events or other lags and is used to create a dimensionless proxy for paleo-wind strength. A proxy for paleo-wind strength was created by subtracting the second order curve from the first order curve (Figure 14c). The first order curve was subtracted to remove the effects that an overall increase in fetch had on the wind energy component in an attempt to isolate wind strength changes through time.

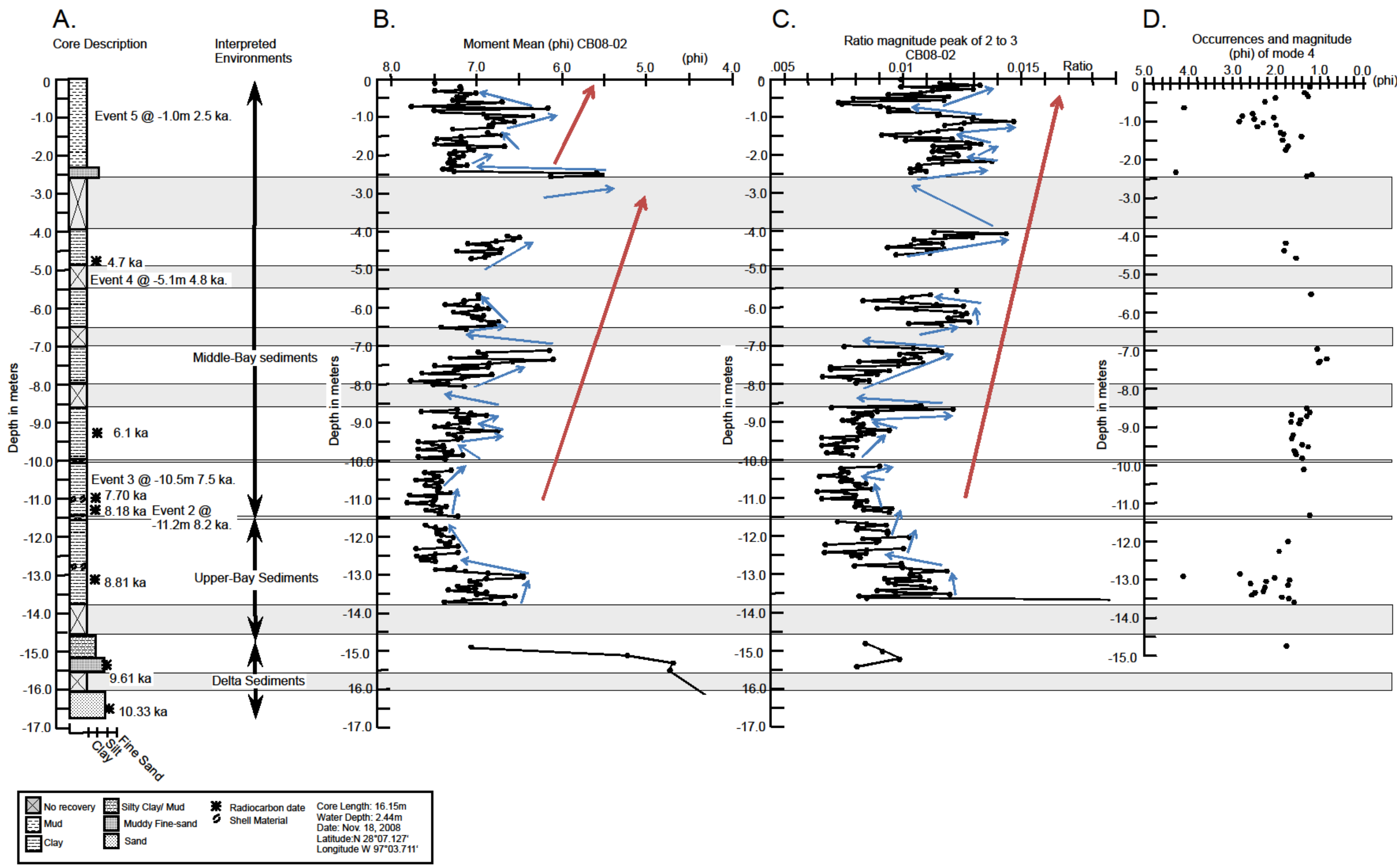


**Figure 14.** **A.** General core description showing interpreted environments for CB08-02, **B.** Grain-size moment mean (phi) for CB08-02, **C.** The ratio between magnitudes of modes 2 and 3 for CB08-02. The larger arrow shows a gradual increase and is thought to represent an increase in fetch as the bay evolved over the last 9.6 ka. The smaller arrow shows a higher frequency and frequency created using the 4$^{th}$ mode within the GSFC suggests that storm deposits. do affect the overall GSFC analyses and are present throughout the studied selection. is thought to represent variable wind strength, **D.** The occurrences and magnitude of the 4$^{th}$ mode are thought to represent storms deposits.

Since the GSFC can also be impacted by storms, we used the presence and/ or absence of this 4th mode to constrain any changes due to changes in storm frequency (figure 14d). The record of storm frequency created using the 4th mode within the GSFC suggests that storm deposits do affect the overall GSFC analyses and are present throughout the studied selection.

Wind proxy data for Copano Bay (Figure 15a) shows a uniform grain-size for 1.2 m above the 8.2 ka flooding event. This was probably a result of the water depth being momentarily out of equilibrium with wind energy dispersion. The disequilibrium caused by a rapid sea-level rise of between 0.4 and 1.2 m (Tornqvist et al., 2004; Kendall et al., 2008) resulted in a uniform aggradation of 1.2 m of bay sediments (Figure 14b and c), which is recorded as relatively low wind strength. The bay reestablished equilibrium around the time of E3 (7.5 ka) flooding event. After E3, wind strength appears to decrease. Isolated indicators of increased wind strength occur at -10.15 m (7.0 ka), -9.20 m (6.12 ka), -8.65 m (5.95 ka), -7.45 m (5.57 ka), 7.15 m (5.48 ka), and -7.10 m (5.46 ka). At each location the accompanying GSFC has a 4th mode and is thought to represent eolian or other coarser suspended deposits delivered to the bay during storms. The occurrence of the 4th mode at an increase in the magnitude between modes 2 and 3 at the same time indicates that the 4th mode does affect the overall ratio. Above -6.5m (5.3 ka), wind strength started to increase. It is believed that prevailing wind strength increased and the change in the grain-size parameter is not due to storm activity. This is based on the absence of the 4th mode and an increase in the ratio between the magnitudes of mode 2 and 3.

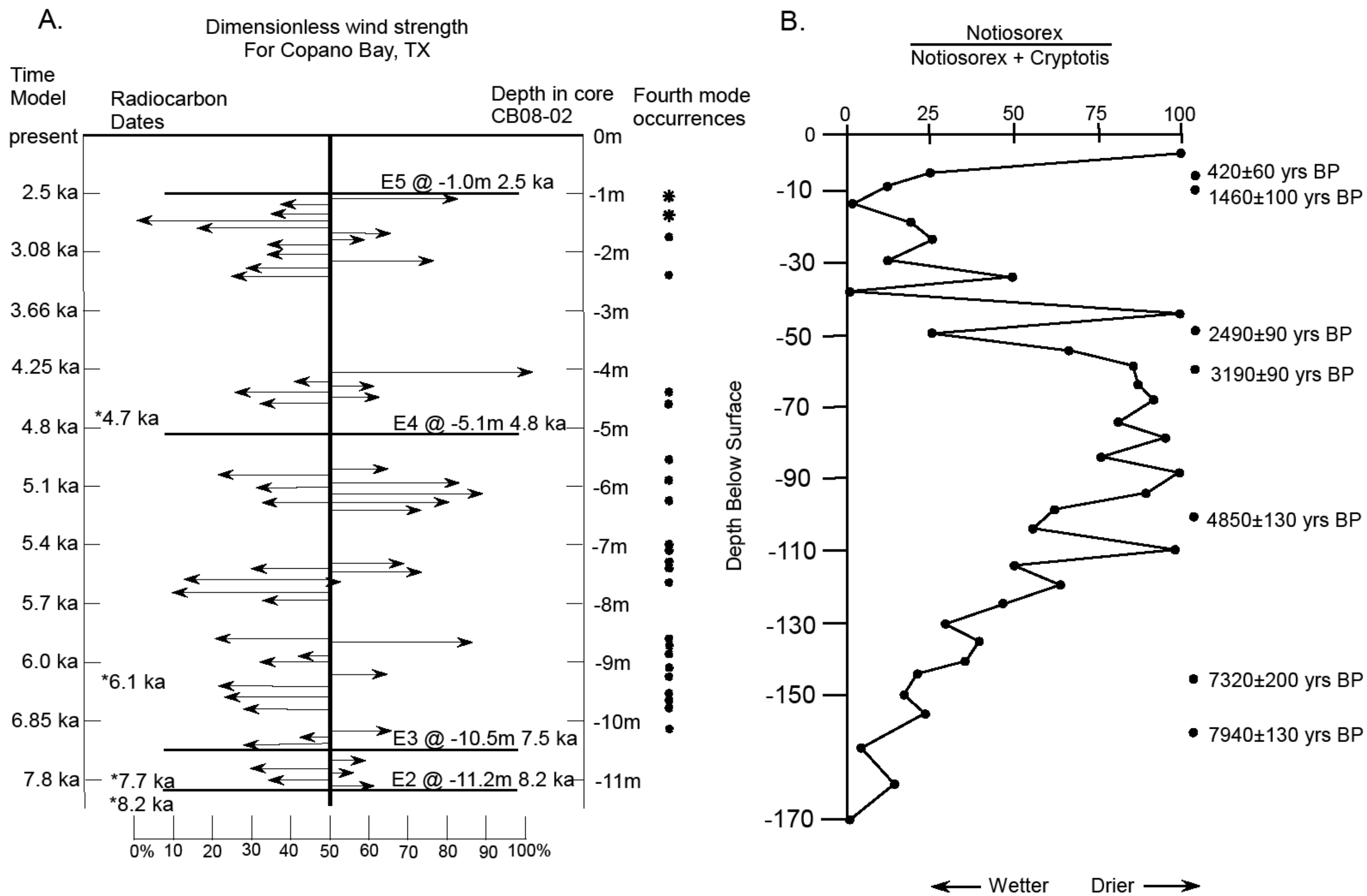


**Figure 15. A.** Dimensionless wind strength proxy for Copano Bay. **B.** The ratio of *Notiosorex* to *Notiosorex* from Toomey et al (1993), which is used as a proxy for wetter or drier climate condition for central Texas.

At -5.1 m (4.8 ka), Event 4, interpreted as a flooding surface, is found. Flooding surfaces were probably accompanied by changes in the hydrodynamics of the bay. This change in the hydrodynamics of the bay is believed to have caused a disruption in sedimentation and is recorded in the grain-size data that appears as a period of calm winds after a flooding surface. This disruption can be seen on our wind strength proxy after the E4 flooding surface (Figure 15a). At -4 m (4.1 ka), proxy data suggest the bay experienced its windiest conditions. This interpretation is based on our wind proxy (Figure 15a). If the disruption to the sedimentary record caused by the flooding surface E4 (4.8 ka) is factored out, from 5.2 to 4.1 ka were the windiest conditions Copano Bay experienced during the Holocene. Toomey et al. (1993) created a climate proxy based on the ratio of *Notiosorex* to *Notiosorex* and *Cryptotis* (Figure 15b); *Notiosorex* are a species of shrews that are more adapted to drier conditions while *Cryptotis* are more adapted to wetter conditions. Toomey et al. (1993) also suggests this time period experienced the driest conditions of the Holocene on the Edwards Plateau. 5.2 ka to 4.1 ka is also the same time period as the controversial middle Holocene highstand. Donnelly and Giosan (2008) suggest that the indicators of a middle Holocene highstand, mostly elevated beach ridges, could be caused by other factors such as increased storminess or wind energy. Our results support their hypothesis.

Our grain-size data suggests that wind strength decreased after -4 m (4.1 ka) to -1.00 m (1.0 ka). After 4.1 ka there are two abrupt spikes in grain-size between -2.45 m (2.45 ka) through -2.35 m (2.35 ka) and -1.10 m (1.1 ka). Both intervals contain a 4$^{th}$ mode and are thought to be the result of storms (Figure 14c and 15a).

In order to provide an independent test of our reconstruction of paleo-wind strength, an attempt was made to correlate our wind proxy with the ratio of *Notiosorex* to *Notiosorex* and *Cryptotis* of Toomey et al (1993) (Figure 15b). The graph of the ratio of *Notiosorex* to *Notiosorex* and *Cryptotis* is used for a proxy to determine wetter or drier climates on the Edwards Plateau (Toomey et al., 1993). During drier climatic conditions, wind velocity would have increased around coastal areas due to a greater temperature differential between ocean and land masses. A reasonable correlation is found (Figure 16).

Our detailed grain-size analysis works well for a proxy record of changes in wind energy between 8.2 ka (E2) and 1.0 ka (E5) in CB08-02. However, the record of wind energy is best preserved between 8.2 ka (E2) and 4.8 ka (E4). After 4.8 ka (E4) the record becomes compressed and might not preserve a record of variation in wind energy as accurately as prior to 4.8 ka. This is because around 4.8 ka the rate of sea-level rise decreases considerably from 1.77 mm/yr. to around 1.3 mm/yr (Simms et al., 2007; Milliken et al., 2008a). The decrease in the rate of sea-level rise slowed accommodation creation to the point that the record starts to become compressed after 4.8 ka (E4).

The record is incomplete before 8.2 ka (E2) because below 8.2 ka (E2) upper-bay deposits are encountered, which are too coarse and are influenced more by fluvial processes rather than wind driven waves and thus are not useful in reconstructing the paleo wind energy.

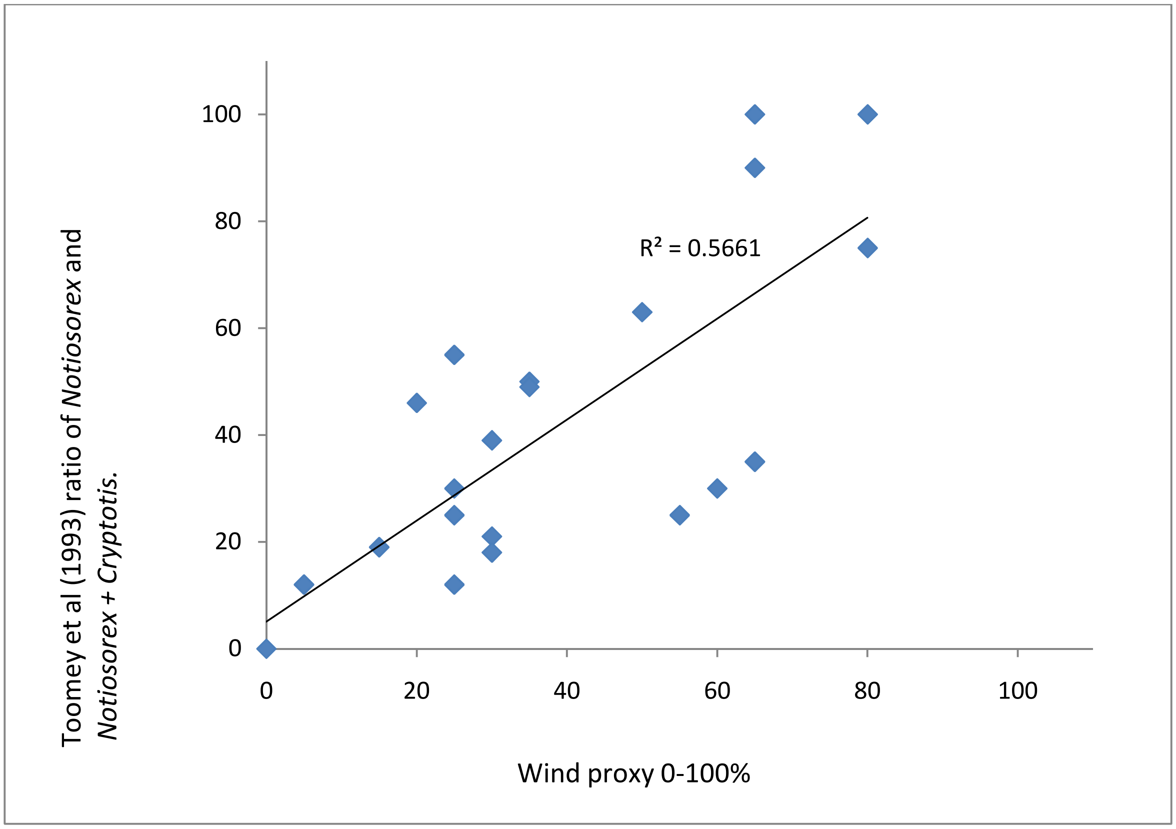


**Figure 16.** Correlation of wind strength proxy for Copano Bay to Toomey et al (1993) ratio of *Notiosorex* to *Notiosorex* and *Cryptotis.*

The record after 1.0 ka (0.5-1.0m) is thought not to be accurate and may not be truly reflective of conditions at the time of deposition but may be influenced by anthropogenic activities such as shipping and dredging that has occurred over the last 100 years. Another important factor for accommodation creation is the amount of compaction that has occurred at the core site CB08-02. Paul and Barras (1998) concluded that the amount of compaction above an incompressible surface is greatest at one-half the depth of the sedimentary column and decreases away from the midpoint. The amount of compaction at the midpoint ranges from 1-10% of the sedimentary thickness (Paul and Barras, 1998). Using Paul and Barras (1998) method, a linear approximation model was created using 5 ± 5% compaction at the midpoint (Figure 17). Based on seismic profiles, the total sedimentary thickness at CB08-02 was found to be 22 m. Estimates for compaction at 4.8 ka (E4) and 1.0 ka (E5) events are 0.125± .125 m and 0.05 ± .05 m respectively based on a linear approximation of Paul and Barras (1998) method. After 1.0 ka the rate of sea-level rise was (1.3mm/yr) (Simms et al., 2007) combined with a total subsidence rate of 0.05 mm/yr.

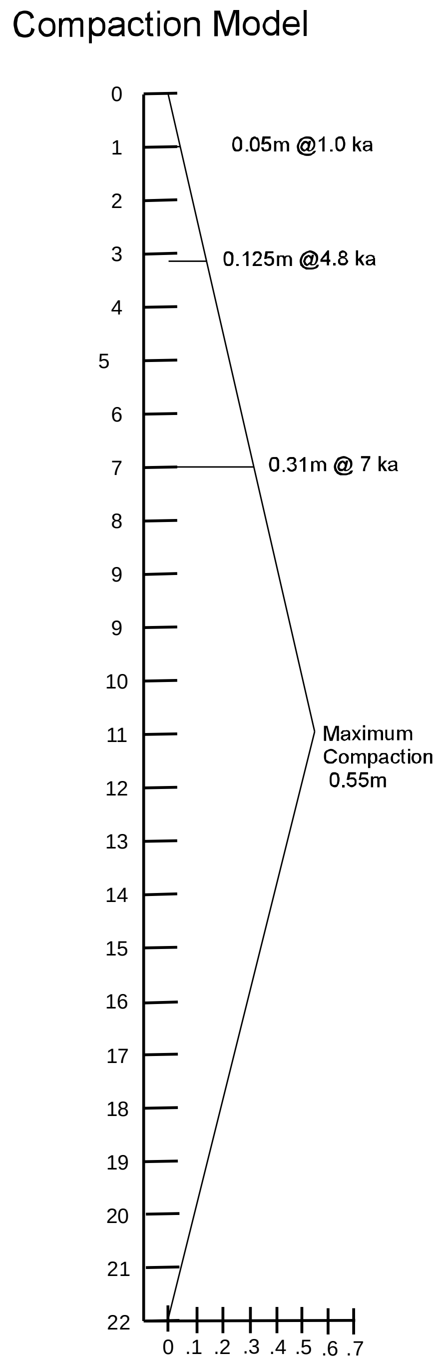


**Figure 17.** Linear compaction model for CB08-02 based on Paul and Barras (1998) midpoint method using 5% compaction at the midpoint.

**Could wind have been a mechanism for a flooding event?**

Wind energy is a powerful agent in regulating sedimentation processes within estuaries. If wind energy did cause a flooding surface, how would it be manifested in the GSFC of the middle-bay deposits? For changes in wind energy to create a flooding surface, wave erosion would have to increase the size of the bay faster than sea-level rise. The only way to increase the size of the bay would be for wind generated waves to erode into the underlying Pleistocene shoreline deposits. Eroding the shoreline would redistribute Pleistocene sediment locally within the bay at the time of the flooding event. The redistributed sediment would be recognized on a grain-size distribution curve as a coarse mode, much like the coarse fluvial modes found in delta-plain deposits. However, these sediments would most likely be constrained to the near shore zone. During time periods of increased wind velocity modes 1 and 2 (M1 and M2) would be greatly reduced due to increased winnowing of bay material of this size. The smaller amount of grains within M1 and M2 should be accompanied by a decrease in sedimentation rates over the interval of the flooding surface. The decrease in sedimentation rates being a result of the export of material being winnowed from the bay. With the reduction of M1 and M2, M3 would increase in proportion as well as modes coarser than 10 μm due to material brought to the bay by eolian processes. Grain-size distribution characteristics described above are not observed at, above, or below any recognized flooding surfaces. However, disruptions to the sedimentary record are observed at recognized flooding events and some of the finest middle bay-deposits are observed. Thus other mechanisms are more likely responsible for the flooding events observed in seismic and cores within Copano Bay.

CHAPTER VI

# CONCLUSIONS

The overall succession of Holocene lithofacies and seismic facies from Copano Bay illustrates a classic transgression. The Holocene sediments record 5 parasequence boundaries or flooding surfaces, which mark major changes to the estuary. The most pronounced of the parasequence boundaries was a large backstepping event that occurred at 8.2 ka due to an estimated sea-level rise of 1.2 m. From the grain-size analysis an overall increase in both the ratio between the magnitudes of mode 2 and 3 and moment mean grain size are believed to be a direct result of wind generated waves winnowing fine sediments and exporting them out of Copano Bay. A disruption in the grain-size trend is seen at the E4 (4.8 ka) parasequence boundaries or flooding surface. This was a result of the bay being momentarily out of equilibrium after the creation of E4 (4.8 ka). A wind proxy for Copano Bay was created from the grain-size data from CB08-02 and correlates well with other proxies for climate over the last 8.2 ka in Texas. The wind strength proxy suggests that Copano Bay experienced its windiest conditions over the last 8.2 ky from 5.2 to 4.1 ka. Wind is a dominant force regulating day-to-day estuarine sedimentary processes. However, grain-size frequency curve at recognized flooding surfaces within middle-bay deposits do not show evidence that the flooding events were caused by increases in wind energy.

REFERENCES


Allen, G.P., 1971. Relationship Between Grain Size Parameter Distribution and Current Patterns in The Girone Estuary. Journal of Sedimentart Petrology, 41(1): 74-88.

Anderson, J., Rodriguez, A., Fletcher, C. and FitzGerald, D.M., 2001. Researchers focus attention on coastal response to climate change. Eos, 82: 513.

Anderson, J.B., Rodriguez, A.B., Milliken, K.T. and Taviani, M., 2008. The Holocene evolution of the Galveston estuary complex, Texas: Evidence for rapid change in estuarine environments. Geological Society Special Publications, *Special Paper 443*, 89-104 pp.

Barber, D.C. et al., 1999. Forcing of the cold event of 8,200 years ago by catastrophic drainage of Laurentide lakes. Nature, 400: 344-348.

Bard, E. et al., 1996. Deglacial sea-level record from Tahiti corals and the timing of global meltwater discharge. Nature London, 382: 244-241.

Blum, M.D., Sivers, A.E., Zayac, T. and Goble, R.J., 2003. Middle Holocene sea-level and evolution of the Gulf of Mexico coast. Journal of Sedimentary Research, 53: 64-77.

Brown, J. et al., 1989. Waves, Tides and Shallow-Water Processes. Oxford, 187 pp.

Bryant, V.M., Jr. and Holloway, R.G., 1985. A late-Quaternary paleoenvironmental record of Texas; an overview of the pollen evidence, 32. Amer. Assoc. Stratigr. Palynologists Found., United States, United States, 39-70 pp.

Calnan, T.R., 1980. Molluscan distribution in Copano Bay, Texas. University of Texas at Austin, Bureau of Economic Geology : Austin, TX, United States, United States, 71 pp.

Clark, P.U. et al., 2001. Freshwater forcing of abrupt climate change during the last glaciation. Science, 293: 283-287.

Cronin, T.M. et al., 2007. Rapid sea level rise and ice sheet response to 8,200-year climate event. Geophysical Research Letters, 34

.Curray, J.R., 1960. Sediments and history of Holocene transgression, continental shelf, northwest Gulf of Mexico, 45, 266-221 pp.

Dalrymple, R.W., Zaitlin, B.A. and Boyd, R., 1992. Estuarine facies models; conceptual basis and stratigraphic implications. Journal of Sedimentary Research, 62: 1130-1146.

Donnelly, J.P. and Giosan, L., 2008. Tempestuous highs and lows in the Gulf of Mexico. Geology, 36: 751-752.

Fairbanks, R.G., 1989. A 17,000-year glacio-eustatic sea level record; influence of glacial melting rates on the Younger Dryas event and deep-ocean circulation. Nature London, 342: 642-637.

Foster-Smith, R.L., 1975. The effect of concentration of suspension on the filtration rates and pseudofaecal production for Mytilus edulis L., Cerastoderma edule (L.) and Venerupis pullastra (Montagu). Journal of Experimental Marine Biology and Ecology, 17(1): 1-22.

Holz, C., Stuut, J.-B.W., Henrich, R. and Meggers, H., 2007. Variability in terrigenous sedimentation processes off Northwest Africa and its relation to climate changes; inferences from grain-size distributions of a Holocene marine sediment record. Sedimentary Geology, 202: 499-508.

Hori, K. and Saito, Y., 2007. An early Holocene sea-level jump and delta initiation. Geophysical Research Letters, 34(18).

Huybrechts, P., 2002. Sea-level changes at the LGM from ice-dynamic reconstructions of the Greenland and Antarctic ice sheets during the glacial cycles. Quaternary Science Reviews, 21(1-3): 203-231.

Kendall, R.A., Mitrovica, J.X., Milne, G.A., Tornqvist, T.E. and Li, Y., 2008. The sea-level fingerprint of the 8.2 ka climate event. In: J.X. Mitrovica, G.A. Milne, T.E. Tornqvist and Y. Li (Editors). Geological Society of America (GSA) : Boulder, CO, United States, United States, pp. 423-426.

Kovacs, J., 2008. Grain-size analysis of the Neogene red clay formation in the Pannonian Basin, Geologische Rundschau = International Journal of Earth Sciences [1999]. Springer International : Berlin, Federal Republic of Germany, Federal Republic of Germany, pp. 171-178.

Lambeck, K., Yokoyama, Y. and Purcell, T., 2002. Into and out of the Last Glacial Maximum: sea-level change during Oxygen Isotope Stages 3 and 2. Quaternary Science Reviews, 21(1-3): 343-360.

Lamp, H., 1945. Hydrodynamics. Dover Publications, New York, 738 pp.

Lightly, R.G., Macintyre, I.G. and Stuckenrath, R., 1982. Acropora Palmata reef framework: A reliable indicator of Sea-level in the Western Atlantic for the past 10,000. Coral Reefs, 1: 125-130.

Lohse, E.A., 1955. A theoretical curve for statistical analysis of sediments, Journal of Sedimentary Petrology. Society of Economic Paleontologists and Mineralogists : Tulsa, OK, United States, United States, pp. 293-296.

Maddox, J. et al., 2008. The Holocene evolution of the Matagorda and Lavaca estuary complex, Texas: Evidence for rapid change in estuarine environments. Special Paper - Geological Society of America, *Special Paper 443*. Geological Society of America (GSA) : Boulder, CO, United States, 105 pp.

Martinez-Andrade, Campbell, P. and Fuls, B., 2005. Trends in relative abundance and size of selected finfishes and shellfishes along the Texas coast. In: T.P.a.W. Department (Editor). Texas Parks and Wildlife Department, Austin, pp. 207-229.

McFarland, E., Jr., 1961. Radiocarbon dating of late Quaternary deposits, south Louisiana. Geological Society of America Bulletin, 72: 158-129.

McGowen, J.H. and Brewton, J.L., 1975. Historical changes and related coastal processes, Gulf and mainland shorelines, Matagorda Bay area, Texas. University of Texas. : Austin, Texas., United States, United States.

Milliken, K.T., Anderson, J.B. and Rodriguez, A.B., 2008a. A new composite Holocene sea-level curve for the northern Gluf of Mexico: Evidence for rapid change in estuarine environments, 443. Geological Society of America (GSA) : Boulder, CO, United States, United States, 1-11 pp.

Milliken, K.T., Anderson, J.B. and Rodriguez, A.B., 2008b. Tracking the Holocene evolution of Sabine Lake through the interplay of eustasy, antecedent topography, and sediment supply variations, Texas and Louisiana: Evidence for rapid change in estuarine environments. Geological Society Special Publications, *Special Paper 443*, 65-88 pp.

Mitchum, R.M., Vail, P.R. and Sangree, J., 1977. Seismic stratigraphy and global changes of sea level; Part 7, Seismic stratigraphic interpretation procedure. Application to Hydrocarbon Exploration Memoir 26. American Association of Petroleum Geologists, Tulsa, OK, 143-135 pp.

Morton, R.A., Paine, J.G. and Blum, M.D., 2000. Responses of stable bay-margin and barrier-island systems to Holocene sea-level highstands, western Gulf of Mexico. Journal of Sedimentary Research, 70: 478-490.

Nelson, H.F. and Bray, E.E., 1970. Stratigraphy and history of the Holocene sediments in the Sabine-High Island area, Gulf of Mexico. Special Publication - Society of Economic Paleontologists and Mineralogists, 15: 77-48.

Nichols, M.M., 1989. Sediment Accumulation Rates and Relative Sea-Level Rise in Lagoons. Marine Geology, 88(3-4): 201-219.

Nordt, L.C., Boutton, T.W., Hallmark, C.T. and Waters, M.R., 1994. Late Quaternary vegetation and climate changes in central Texas based on the isotopic composition of organic carbon. Quaternary Research, 41: 109-120.

Paine, J.G., 1993. Subsidence of the Texas coast: inferences from historical and late Pleistocene sea levels. Tectonophysics, 222(3-4): 445-458.

Paul, M.A. and Barras, B.F., 1998. A geotechnical correction for post-depositional sediment compression; examples from the Forth Valley, Scotland. Journal of Quaternary Science, 13: 171-176.

Pichevin, L., 2005. A 190 ky record of lithogenic grain-size on the Namibian slope; forging a tight link between past wind-strength and coastal upwelling dynamics. Marine Geology, 218: 81-96.

Price, W.A., 1947. Equilibrium of form and forces in tidal basins of coast of Texas and Louisiana. Bulletin of the American Association of Petroleum Geologists, 31: 1663-1619.

Rodriguez, A.B., Anderson, J.B. and Simms, A.R., 2004. Incised-valley fill parasequence formation and implications for estuarine evolution; Galveston Estuary, Texas. In: J.B. Anderson and A.R. Simms (Editors), Abstracts with Programs - Geological Society of America, Denver, CO, United States. Geological Society of America (GSA) : Boulder, CO, United States, United States, pp. 300-300.

Rodriguez, A.B., Anderson, J.B. and Simms, A.R., 2005. Terrace inundation as an autocyclic mechanism for parasequence formation; Galveston Estuary, Texas, U.S.A. Journal of Sedimentary Research, 75: 620-608.

Shepard, F.P., 1956. Rate of postglacial rise of sea level. Science, 123: 1083-1082.

Shepard, F.P. and Moore, D.G., 1954. Sedimentary environments differntiated by coarse-fraction studies. Bulletin of the American Association of Petroleum Geologists, 38: 1802-1792.

Shideler, G.L., 1984. Suspended sediment responses in a wind-dominated estuary of the Texas Gulf Coast. Journal of Sedimentary Research, 54: 745-731.

Simms, A., Aryal, N., Yusuke, Y., Hiroyuki, M. and Regina, D., 2009. Insights on a Proposed Mid-Holocene Highstand Along The Northwestern Gulf of Mexicao From the Evolution of Small Coastal Ponds. Journal of Sedimentary Petrology, 79: 757-772.

Simms, A.R., Anderson, J.B. and Rodriguez, A.B., 2008. Mechanisms controlling environmental change within an estuary; Corpus Christi Bay, Texas: Evidence for rapid change in estuarine environments. Special Paper - Geological Society of America, 443. Geological Society of America (GSA) : Boulder, CO, United States, United States, 121-146 pp.

Simms, A.R., Lambeck, K., Purcell, A., Anderson, J.B. and Rodriguez, A.B., 2007. Sea-level history of the Gulf of Mexico since the Last Glacial Maximum with implications for the melting history of the Laurentide Ice Sheet. Quaternary Science Reviews, 26(7-8): 920-940.

Sperazza, Michael, M., N., J. and Hendrix, M.S., 2004. High-resolution particle size analysis of naturally occurring very fine-grained sediment through laser diffractometry. Journal of Sedimentary Research, 74: 736-743.

Stuiver, M. and Reimer, P.J., 2005. CALIB Radiocarbon Calibration 5.0.2., CALIB Radiocarbon Calibration 5.0.2. http://calib.qub.ac.uk/calib/.

Stuut, J.-B. et al., 2005. Provenance of present-day eolian dust collected off NW Africa. 110.

Thomas, E.R. et al., 2007. The 8.2 ka event from Greenland ice cores. Quaternary Science Reviews, 26: 70-81.

Thomas, M.A. and Anderson, J.B., 1994. Sea-level controls on the facies architecture of the Trinity/Sabine incised-valley system, Texas continental shelf. Special Publication - Incised-valley systems, 51. SEPM (Society for Sedimentary Geology) : Tulsa, OK, United States, United States, 63-82 pp.

Thornthwaite, C.W., 1948. An approach toward a rational classificaion of climate. Geolgraphical review 38(1): 55-94.

Toomey, R.S., III, Blum, M.D. and Valastro, S., Jr., 1993. Late Quaternary climates and environments of the Edwards Plateau, Texas. Global and Planetary Change, 7: 320-299.

Tornqvist, T.E., Bick, S.J., Gonzalez, J.L., van der Borg, K. and de Jong, A.F.M., 2004. Tracking the sea-level signature of the 8.2 ka cooling event; new constraints from the Mississippi Delta. Geophysical Research Letters, 31(23): 4 pp.

Wright, S.S., 1980. Seismic Stratigraphy and Depositional History of Holocene Sediments on the Central Texas Gulf Coast. Master's Thesis, The University of Texas at Austin Austin, TX, 123 pp.

Yu, S.-Y., Berglund, B.E., Sandgren, P. and Lambeck, K., 2007. Evidence for a rapid sea-level rise 7600 yr ago. Geology, 35: 891-894.

## ABSTRACT

Over 123 km of high-resolution 2-D seismic lines and 6 sediment cores up to 16 m in length were collected from Copano Bay along the northwestern Gulf of Mexico in order to investigate the role wind energy had on the evolution of Copano Bay, Texas over the last 10 ka. Paleo-geographic maps of the bay were constructed with the use of seismic profiles and core data to show how the bay evolved through time. Five environmental changes are observed within Copano Bay over the last 9.6 ka. The largest environmental change occurred at 8.2 ka. At the 8.2 ka event, estimates suggest that the bayhead delta back-stepped about 7.5 km resulting from a sea-level rise of 1.2 m at that time. Using grain-size data from middle-bay deposits, a proxy for wind strength is also produced. The wind strength proxy is correlated with other published paleo-climatic records for the area and a reasonable correlation is found. From the grain-size derived wind strength proxy, it is suggested that Copano Bay experienced its windiest conditions of the past 8.2 ky from 5.2 to 4.1 ka. Wind is a dominant force regulating estuarine sedimentary processes. However, grain-size frequency curves at recognized environmental changes within middle-bay deposits do not show evidence that environmental changes were brought on by increases in wind energy.

VITA

Benjamin Taylor Troiani

Candidate for the Degree of

Master of Science

Thesis: AN INVESTIGATION OF CHANGING WIND ENERGY ON THE EVOLUTION OF COPANO BAY, TEXAS

Major Field: Master of Science in Geology

Biographical:

Personal Data:
Born: September 13th, 1979 in San Antonio, Texas
Parents: Gay and Lende Troiani

Education:
B.S. Wichita State University, Wichita, Kansas in December, 2006.
M.S. Oklahoma State University, Stillwater, Oklahoma in December, 2009.

Experience:
Contract Geologist Pogo Exploration and Producing, Tulsa, OK (2007-2008)
Geologic Intern Kirkpatrick Oil Company, Oklahoma City, OK (summer of 2008)
Geologic Intern Devon Energy, Oklahoma City, OK (summer of 2009)

Professional Memberships:
American Association of Petroleum Geologist (AAPG)
The Geological Society of America (GSA)
Society for Sedimentary Geology (SEPM)
Oklahoma City Geological Society member

Name: Benjamin Taylor Troiani Date of Degree: Spring 2010

Institution: Oklahoma State University Location: Stillwater, Oklahoma

Title of Study: AN INVESTIGATION OF CHANGING WIND ENERGY ON THE EVOLUTION OF COPANO BAY, TEXAS

Pages in Study: 61 Candidate for the Degree of Master of Science

Major Field: Geology

Scope and Method of Study:

The aim of this study was to see if paleo-wind energy had an effect on the evolution and sedimentology of Copano Bay, Texas. To achieve this I acquired 6 sediment cores and over 123 km of 2-D seismic lines. I made paleo-geographic maps of the bay through time and conducted a detailed grain-size analysis of the cores. From the grain-size data I produced a proxy for wind strength and correlated my findings with other published paleo-climatic records for the area.

Findings and Conclusions:

Five environmental changes were recognized within Copano Bay since the Last Glacial Maximum. Four of the environmental changes were back-stepping events and the fifth was the bay changing to its current configuration. The largest back-stepping event took place at 8.2 ka. At 8.2 ka sea-level rose about 1.2 m. The wind strength proxy suggests that the windiest conditions within Copano Bay occurred over the last 8.4 ky from 5.2 to 4.1 ka. This interpretation is based on the newly created wind strength proxy and other published climatic records. It appears that changes in wind energy alone did not cause parasequence boundaries or flooding events within Copano Bay.

ADVISER'S APPROVAL: Dr. Alexander Simms